Computational simulation of Acrylamide and Acrylic Acid reaction by free-radical copolymerization in different reactor configurations and thermal conditions.

by

Diego A. Bugaiov Azurica

A report submitted to the Faculty of Graduate Studies and Research and the Faculty of Engineering in partial fulfillment of the requirements for the degree of

Master of Engineering

in

Chemical Engineering

Supervisor – Dr. Joao Soares

Date – March 2020.

Department of Chemical and Materials Engineering

University of Alberta

Executive Summary

This study simulates the free-radical copolymerization of acrylamide and acrylic acid. The simulations were carried out for different reactor configurations and thermal conditions. Moreover, final copolymer microstructure was predicted by using mathematical simulations based on first principles. Although there are great amount of publications about the modelling of polymer reactions, this work aims to estimate the final copolymer microstructure at the end of conversion using a method with lower computational efforts. Those values will determine important properties, among others, physical and chemical behaviours in later copolymer applications. A study of how natural disturbances affect the copolymer properties has been analyzed too. Finally, a controller was implemented to control the temperature reaction as the input variable.

All the simulations were carried out using the software MATLAB®. Aqueous solutions were considered, and the initial monomer concentration for all the simulations was 15 % wt. Seven different cases were simulated, where the first two were batch reactors with isothermal and adiabatic conditions, respectively. The third and fourth cases were semi-batch reactors with isothermal and adiabatic conditions, respectively. Finally, the last three cases were the simulations in a semi-batch reactor with isothermal conditions but, considering that the monomer's inflow presented disturbances. Our results point that when the temperature varies as a function of time, the average chain length decreases. Furthermore, in all the models, the average molecular weight is bigger than 10^3. Hence, the error's method is lower or equal than 5%. Copolymer composition distribution is broader for batch than semi-batch configuration. The larger is the variance of the white noise, the broader is the copolymer composition distribution.

It is concluded that the best configuration to produce a narrow distribution for both, copolymer composition and molecular weight distribution, is the isothermal semi-batch reactor. However, great control in the monomer inflow should be implemented to avoid composition drift in the copolymer microstructure.

Table of Contents

List of Tables

List of Figures

1. Introduction

Polymers have a tremendous impact on our daily life and society, from the production of medical supplies that could be used to fight against a pandemic, the packaging that our food is delivered in or the development of novel materials such as nanomaterials. Polymers play a crucial role in our economy and environment. With consideration to the latter, sustainable production is necessary to ensure a better world for the ones to come. The production process could be improved if we can understand the core of the polymer reactions, where different physical phenomena are happening currently. Pertinent processes include the production of polymers and copolymers (polymerizations in which more than one monomer is reacting) by free radical polymerization (FRP). FRP is a type of reaction conducted by the formation of free radicals that react with the monomers to produce long polymer chains. Both, process control and a deeper understanding of the process can improve the sustainability of the process by ensuring a safe process, reduce undesired wastes and improve the revenue.

With the goal of improving the sustainability of the process, the objective of this project is the modelling and simulation of a free radical copolymerization reaction in aqueous solution, especially between Acrylic Acid (AAc) and Acrylamide (AAm) as monomers. Aqueous solution reactions are important because are more friendly with the environment and much safer for the people that will be manipulating the operation. Simulations for an isothermal and adiabatic batch and semi-batch reactor configuration are conducted. Then, estimation of the final microstructural properties such as chemical composition and molecular weight distribution at final conversion is calculated and compared to the previous work of some authors. [2-7,13,14]

However, the previous work has not predicted and determined the microstructure for this copolymerization. Moreover, we analyze what effects disturbances have on the desired copolymer microstructure of the copolymer.

The main goals of this present work described in this report were the following:

1. Develop a mathematical model for the copolymerization in aqueous solution between AAc and AAm in a batch and semi-batch reactor configurations.
2. Study how isothermal and adiabatic conditions for both types of reactors affect the process.
3. Calculate the copolymer microstructure for all the simulations using PKRCM and the method of moments.
4. Analyze how the presence of disturbances in the inflow feed affects the final copolymer microstructure.
5. Implement a PD controller to control the reactor temperature in a semi-batch reactor situation.

2. Literature Review

Recently, the development of new materials has taken on important significance due to the various unique demands that the industry must satisfy. Daily experiments are carried out to make new materials with specific physical and chemical properties. We rely on different methods such as polymerization reactions, to develop these novel materials. Polymers are widely used and play important roles in a variety of industries that range from cosmetics to nanotechnology. They have shaped our life because of their extraordinary versatility brought about by customizable properties that stem from their complex microstructural features. One process to make polymers is the copolymerization reaction, where two different reagents (monomers) are mixed in the presence of an initiator and solvent to make a copolymer. The properties of this copolymer will be defined by the molecular and morphological characteristics of the copolymer itself, how the copolymer was processed, and the additives used for compounding the copolymer.[1] However, the final structure is incredibly complex. So much so that major research continues into the prediction of this final structure due to major implications a model could have on economic savings, process control and reducing operational risks. One methodology to predict the final polymer properties is to use first principles modelling. Nevertheless, the model results could be misinterpreted because we usually attribute inaccuracy with the mathematical model instead of the proper interpretation of the process.[2]

So, why would a model be so important? We can mention different reasons to highlight why mathematical modelling could be very useful, but the following are considered the more relevant.[2]

1. Models enhance our process understanding, act as a reservoir of knowledge about a process. They can reveal interactions within the process that may be impossible to detect from direct measurement.
2. Models are useful for process design, parameter estimation and process simulation. Also, they are critical to the implementation of any controller or automation in the process. They also have cost-effectiveness implications.
3. Models are needed for process optimization, especially when the process is nonlinear and when the number of constraints could be considerable.
4. Models are useful for safety considerations too. We can extrapolate or simulate different situations in the process and investigate possible effects on the process factors.
5. Models are useful for the education and training of new personnel in any industry.

Several works modelling a polymer reaction processes have been published for over 40 years. Often in these papers, one of the main objectives is the prediction of the final polymer microstructure which later determine the physical and chemical polymer properties (Ray, 1972; Kiparissides, C., et al., 1979; Pendelis et al., 1985; Hameliec et al. 1987; Rawiling and Ray, 1988).[14, 16, 13, 5, 15] One of the first copolymer simulations published was the work of Hamer et al. (1981), where they studied the dynamic behaviour of vinyl acetate and methylmethacrylate copolymerization reaction in a continuous stirred tank reactor (CSTR). They determined how process characteristics such as feed monomer flows or reactor cooling capacity allow multiple steady states and how the use this information could predict undesired dynamic behaviours.[3] T. O. Broadhead et al. (1985) presented the modelling of Styrene/Butadiene by emulsion

polymerization in a batch, semi-batch and continuous reactor where they predicted copolymer properties such as the number and weight molecular weight averages and monomer composition with a good estimation of the model parameters.[4] Nevertheless, our interest is in free radical polymerization, a type of polymerization technique that is versatile, of synthetic efficiency and great compatibility with a wide variety of functional groups. It is said that radical polymerization has witnessed a renaissance in terms of mechanistic knowledge and synthetic possibilities. One of the forces that have driven to this renaissance is the growing demand for purpose-built materials for nanotechnology.[17] Before moving on, we briefly explain the free radical polymerization process and its implications below.

2.1. Free Radical Polymerization

Typically, the free radical polymerization consists of three different steps: initiation, propagation and termination.[1] The initiation consists on the free radical (I^*) generation from an initiator (I) that will later react with the monomer molecules (M) to start a chain. The process may be represented in the following reactions:

$$I \xrightarrow{k_d} 2I^*$$

$$I^* + M \xrightarrow{k_I} M^*$$

The propagation step is the addition of the free radical monomer to a monomer unit that produce another free radical monomer unit but with two or more monomers.

$$M^* + M \xrightarrow{k_p} M - M^*$$

$$M - M^* + M \xrightarrow{k_p} M - M - M^*$$

$$M_{n-1}^{*} + M \overset{k_p}{\rightarrow} M_n^{*}$$

Reaction between a free radical monomer with other radical, solvent, initiator or with the own radical chain could be happening in parallel of the propagation step.

Finally, the termination step consists of the combination of two living chains (the ones that contain a free radical molecule) to produce a dead chain. This could happen by combination or disproportionation and both cases are represented in the following equations.

By combination

$$M_n^{*} + M_m^{*} \overset{k_{tc}}{\rightarrow} D_{n+m}$$

By disproportionation

$$M_n^{*} + M_m^{*} \overset{k_{td}}{\rightarrow} D_n + D_m$$

As we have mentioned, the free radical polymerization process has been well studied and all the parameters and factors could be precisely determined by Steady-State assumptions.[1]

For a free radical copolymerization process, the presence of at least two different kinds of monomers will count for propagation, termination and transfer reaction rates. Most of the mentioned authors consider that the reactivity chain depends only on the last monomer added (terminal effect). This assumption allows us to define the kinetic rate based on the last monomer added instead of the overall composition of the living chain. Moreover, the tendency of two monomers to react together is a difficult relation to quantify that usually depends on the solvent, monomers, initiator and concentrations. The simplest model studied in this work is presented by

Mayo and Lewis, where they have stated that the copolymerization of two monomers leads to two types of free radical monomers.[23] Therefore, there are four possible reactions for the overall propagation:

$$M_1^* + M_1 \xrightarrow{k_{p11}} P_1^*$$

$$M_1^* + M_2 \xrightarrow{k_{p12}} P_2^*$$

$$M_2^* + M_1 \xrightarrow{k_{p21}} P_1^*$$

$$M_2^* + M_2 \xrightarrow{k_{p22}} P_2^*$$

Where $k_{p11}, k_{p12}, k_{p21}$ and k_{p22} are rate constants of the individual propagation reactions and P_1^* and P_2^* represent the living chain with terminal radical monomer 1 and 2 respectively. Based on the above equations, the reactivity ratios (r_1, r_2) are defined as the ratios of the constant of cross-propagation for each of the monomers.

$$r_1 = \frac{k_{p11}}{k_{p12}}$$

$$r_2 = \frac{k_{p22}}{k_{p21}}$$

A.E. Hameliec et al. (1987) published one of the first papers that includes complete and general aspects in the designing and modelling of multicomponent free-radical polymerization in batch, semi-batch and continuous reactors. They developed a practical methodology for the generic computational modelling of multicomponent free radical polymerization for a solution and emulsion systems for any monomers. [2,5] In our case, the discussion will be center on a free

radical solution polymerization where the solvent is water and all the reaction steps proceed in a single phase. A model reactor will be based on a set of material balances for all the components describing the rates of accumulation, outflow, inflow and disappearance by the reaction. The balances will be later used to calculate the conversion, composition and other polymer properties. Though this work does not mention in detail how to evaluate the moment equations to complete the set of ordinary differential equations that represent the whole model, Xie, T. et al. (1993) published an elegant method to describe the copolymerization behaviour of linear copolymers formed in a batch reactor. They used a method named "pseudo-kinetic rate constant method" (PKRCM) used to calculate the molecular weight distribution (MWD) for multicomponent polymerization producing linear chains. They have concluded that the error of this method is less than 5 % when the number-average molecular weight is greater than 10^3, and a Stockmayer's bivariate distribution could be obtained by a batch or semi-batch reactor. [6,7,24]

Another essential factor to determine is each of the reactivity ratios for the monomers under aqueous conditions. Most of the authors mentioned have reported correlations for these parameters, but the relations are quite scattered and dissimilar. [19 - 22] The effect of the pH, ionic strength, reagents concentrations, temperature, solvent and initiator affect the reactivity ratios, and reliable estimation of those relations will be critical for the correct prediction of the copolymer microstructure. Rintoul, I. et al. (2005); Riahinezhad, M., et al. (2013) and Preusser, C., et al. (2016) reported a correlation for both relations that are easily implemented into a model, and are based on experimentally measured composition over a great range of pH and ionic strength conditions.[8,18,19] To design a well-developed model, all the correlations and

equations implemented have to be accurate and reliable, allowing us to get a closer estimation of the correct copolymer microstructure.

As we have mentioned before, copolymers are significant due to their extraordinary properties that monomers cannot match, and the final product may have a great variety of applications. The copolymer being studied is especially interesting; is one of the most important soluble copolymers which are widely used in applications such as flocculants for wastewater treatment, drag reductions agents, textile formulation processing aids, adhesives, cosmetics and enhanced oil recovery (EOR).[8,11] There is a special interest in this copolymer for EOR because it may meet the requirement of highly viscous, aqueous solution with mechanical and thermal stability.[9,10] In addition, these copolymers are finding some applications in treatment of oil sand tailing ponds in Western Canada.[11] Also, because the copolymerization of this compound is made in aqueous solution, it is an attractive way of production due to its environmentally friendly properties and inexpensive solvent cost.[12]

The mathematical modelling and numerical solution of this copolymerization have not been reported yet, and this work intends to develop a model to predict the copolymer microstructure for different reactor configurations at different conditions. Because of its complexity and all the applications that this copolymer can be used for, the mathematical modelling and simulation in various reactor configurations and conditions make it a fascinating case for study.

3. Problem Statement and Method

We start our problem statement or in this case, model development, by presenting the chemical equations that characterize this binary copolymerization. Then, the different material balances for each of the components and the reactor heat balance will be discussed with a briefly explanation for different reactor configurations. Finally, we introduce the moment equations and how the final copolymer microstructure properties will be affected by them.

3.1. Chemical Equations

In the following equations, I is the initiator, P_i^* is a radical chain ending on monomer type i, M_i is the monomer type i and D are the dead chains. In our study, Monomer 1 (M_1) is Acrylamide (AAm) and Monomer 2 (M_2) is Acrylic Acid (AAc).

Initiation

$$I \xrightarrow{k_d} 2I^*$$

$$I^* + M_1 \xrightarrow{k_{I1}} P_1^*$$

$$I^* + M_2 \xrightarrow{k_{I2}} P_2^*$$

Propagation

$$M_1^* + M_1 \xrightarrow{k_{p11}} P_1^*$$

$$M_1^* + M_2 \xrightarrow{k_{p12}} P_2^*$$

$$M_2^* + M_1 \xrightarrow{k_{p21}} P_1^*$$

$$M_2^* + M_2 \xrightarrow{k_{p22}} P_2^*$$

Chain transfer to monomer

$$P_1^* + M_1 \xrightarrow{k_{f11}} D_1 + P_1^*$$

$$P_1^* + M_2 \xrightarrow{k_{f12}} D_1 + P_2^*$$

$$P_2^* + M_1 \xrightarrow{k_{f21}} D_2 + P_1^*$$

$$P_2^* + M_2 \xrightarrow{k_{f22}} D_2 + P_2^*$$

Termination

By combination

$$P_1^* + P_1^* \xrightarrow{k_{tc11}} D_{1+1}$$

$$P_1^* + P_2^* \xrightarrow{k_{tc12}} D_{1+2}$$

$$P_2^* + P_1^* \xrightarrow{k_{tc21}} D_{2+1}$$

$$P_2^* + P_2^* \xrightarrow{k_{tc22}} D_{2+2}$$

By disproportionation

$$P_1^* + P_1^* \xrightarrow{k_{td11}} D_1 + D_1$$

$$P_1^* + P_2^* \xrightarrow{k_{td12}} D_1 + D_2$$

$$P_2^* + P_1^* \xrightarrow{k_{td21}} D_2 + D_1$$

$$P_2^* + P_2^* \xrightarrow{k_{td22}} D_2 + D_2$$

We would like to mention some simplifications that have been considered to develop a simpler model. We are not considering the presence of water-soluble impurities that may react with an initiator or other free radical molecules, we are considering only linear polymer formation, i.e., we are not contemplating a possible transfer to polymer reactions which could lead to cross-linking and branching copolymer structures. Backbiting is also not considered, and we are neglecting the presence of any chain transfer agent in solution.

3.2. Material Balances

Material balances in a semi-batch reactor for all the main species and the reaction volume variation are presented. The balances for a batch copolymerization reactor are obtained by eliminating any inflow term in each of the material balances.

Monomer Balances

$$\frac{dN_1}{dt} = F_{N_1,in} - R_{p1}V$$

$$\frac{dN_2}{dt} = F_{N_2,in} - R_{p2}V$$

$N_1, N_2 =$ moles of monomer 1 and 2 in the reactor.

$F_{N_1,in}, F_{N_2,in} =$ molar flow of monomers into the reactor.

$V =$ reacting volume in the reactor.

$R_{p1}, R_{p2} =$ net disappearance rate of monomer by reaction.

Reaction Volume

$$\frac{dV}{dt} = \left(F_{N_1,in}\frac{MW_{M_1}}{\rho_{M_1}} + F_{N_2,in}\frac{MW_{M_2}}{\rho_{M_2}}\right) - \left[R_{p1}MW_{M_1}\left(\frac{1}{\rho_{M_1}} - \frac{1}{\rho_P}\right) + R_{p2}MW_{M_2}\left(\frac{1}{\rho_{M_2}} - \frac{1}{\rho_P}\right)\right]V$$

$MW_{M_1}, MW_{M_2} =$ molecuar weight of the monomers.

$\rho_{M_1}, \rho_{M_2}, \rho_P =$ densities of the monomers and the polymer.

Polymer Balances

$$\frac{dP_1}{dt} = F_{P_1,in} + R_{p1}V$$

$$\frac{dP_2}{dt} = F_{P_2,in} + R_{p2}V$$

$P_1, P_2 =$ moles of monomers 1 and 2 bound as polymer in the reactor.

$F_{P_1,in}, F_{P_2,in} =$ monomer inflow into the reactor bound as polymer.

Additional Balances

$$\frac{dN_I}{dt} = F_{N_I,in} - R_{pI}V$$

$$\frac{dN_S}{dt} = F_{N_S,in}$$

$N_I, N_S =$initiator and solvent moles in the reaction volume.

$R_{pI} =$initiator disappearance rate.

Heat Balance

$$\frac{d\left(\sum_j M_j Cp_j\left(T - T_{ref}\right)\right)}{dt} = \sum_i F_{N_i,in} Cp_i\left(T_{in} - T_{ref}\right) + \sum_i R_{p,i}\left(-\Delta H_{p,i}\right)V$$

Cp =heat capacity of the specie.

M = specie mass.

T = reactor temperature.

T_{in} = inflow stream temperature.

$\Delta H_{p,i}$ = heat of polymerization of monomer i.

3.3. Method of Moments for binary copolymerization

Ray, W. (1972), developed a complete description of the moment equations for both homopolymerization and copolymerization to obtain, among others, the number and weight average molecular weight with different mathematical techniques. This method could be tedious and may consume more computing efforts because it requires solving a system of over 14 ordinary differential equations. Though, Xie, T. et al. (1993) proposed a new approach for solving the problem by making kinetic simplifications, and was named “Pseudo-kinetic rate constant method” (PKRCM). This method applies the well-known homopolymerization moment equations in a copolymerization model by redefining the global rate constants. Consequently, the method is much more manageable, and its error could be less than 5 % when the average molecular weight is larger than 10^3. The final versions of the moment equations are presented as following but a detailed deduction could be found in [7].

The moments for live and dead copolymer chain distributions are defined

$$Y_{ij} = \sum_{m=0}^{\infty}\sum_{n=0}^{\infty}(mM_1 + nM_2)^j\left[P^*_{m,n,i}\right] \ (i = 1,2, \dots j = 0,1,2, \dots)$$

$$Q_k = \sum_{m=0}^{\infty}\sum_{n=0}^{\infty}(mM_1 + nM_2)^k\left[D_{m,n}\right] \ (k = 0,1,2, \dots)$$

Where Y_{ij} is the j[th] moment of copolymer radical chain distribution of type i and Q_k is the k[th] moment of dead copolymer chain distribution.

Now, we introduce PKRCM which defines the propagation rate as follows

$$R_p = k_{p11}[M_1][P_1^*] + k_{p12}[M_1][P_2^*] + k_{p21}[M_2][P_1^*] + k_{p22}[M_2][P_2^*]$$

Where $[P_1^*] = \sum_{r=1}^{\infty}\left[P^*_{r,1}\right]$ and $[P_2^*] = \sum_{r=1}^{\infty}\left[P^*_{r,2}\right]$.

Defining

$$f_i = \frac{[M_i]}{\sum_{i=1}^{2}[M_i]}$$

$$\phi_i = \frac{[P_i^*]}{\sum_{i=1}^{2}[P_i^*]}$$

The propagation rate could be rewritten as follows

$$R_p = \overline{k_p}[M][P^*]$$

Where

$$[M] = \sum_{i=1}^{2}[M_i]$$

$$[P^*] = \sum_{i=1}^{2} [P_i^*]$$

$$\overline{k_p} = \sum_{i=1}^{2} \sum_{j=1}^{2} k_{pij} \phi_i f_j$$

Similarly, the termination rate could be expressed as

$$R_t = \overline{k_t} [P^*]^2$$

Where

$$\overline{k_t} = \overline{k_{td}} + \overline{k_{tc}}$$

$$\overline{k_{td}} = \sum_{i=1}^{2} \sum_{j=1}^{2} k_{tdij} \phi_i \phi_j$$

$$\overline{k_{tc}} = \sum_{i=1}^{2} \sum_{j=1}^{2} k_{tcij} \phi_i \phi_j$$

In this work, gel effect is not considered because it is a solution polymerization and the total monomer fraction will not exceed 15 %. If a bulk copolymerization is simulated, then other global constants for the complete process will be considered due to diffusion-controlled phenomena at high monomer conversions.[2]

From the classical quasi-steady state assumption (QSSA) [1], we know that

$$R_t = R_{pI}$$

Which leads to the well-known concentration expression for the total polymer living chains

$$[P^*] = \left(\frac{R_{pI}}{\overline{k_t}}\right)^{0.5} = \left(\frac{2fk_d[I]}{\overline{k_t}}\right)^{0.5}$$

And the propagation rate is defined as

$$R_p = \overline{k_p}[M]\left(\frac{2fk_d[I]}{\overline{k_t}}\right)^{0.5}$$

For the transfer to monomer reactions, we can also define a pseudo-kinetic constant as

$$\overline{k_f} = \sum_{i=1}^{2}\sum_{j=1}^{2} k_{fij}\phi_i f_j$$

Considering that the variation respect to time for both of the living chain concentration is zero and neglecting the other terms, we can obtain the following expression

$$\frac{d[P_1^*]}{dt} \approx k_{p21}[P_2^*][M_1] - k_{p12}[P_1^*][M_2] = 0$$

$$\frac{[P_1^*]}{[P_2^*]} = \frac{k_{p21}[M_1]}{k_{p12}[M_2]}$$

So, we can get an expression for ϕ_i as

$$\phi_1 = \frac{k_{p21}f_1}{k_{p21}f_1 + k_{p12}f_2}$$

$$\phi_2 = \frac{k_{p12}f_2}{k_{p21}f_1 + k_{p12}f_2}$$

Assuming that the mole fraction of radical is independent of polymer chain length, we can consider that throughout the whole reaction, the radical fraction could be calculated with the

above expressions. The moment equations for homopolymerization have already been developed and are presented as follows [25]

$$\frac{dQ_0}{dt} = R_p \cdot \left(\tau + \frac{\beta}{2}\right)$$

$$\frac{dQ_1}{dt} = R_p$$

$$\frac{dQ_2}{dt} = R_p \cdot \frac{(2 \cdot \tau + 3 \cdot \beta)}{(\tau + \beta)^2}$$

Where

$$\tau = \frac{\overline{k_{td}}[P^*]}{\overline{k_p}[M]} + \frac{\overline{k_f}}{\overline{k_p}}$$

$$\beta = \frac{\overline{k_{tc}}[P^*]}{\overline{k_p}[M]}$$

Instantaneous number and weight molecular weights can be expressed as

$$M_n(t) = \frac{M_{av}(t)}{\left(\tau + \frac{\beta}{2}\right)}$$

$$M_w(t) = M_{av}(t)\frac{(2 \cdot \tau + 3 \cdot \beta)}{(\tau + \beta)^2}$$

$$M_{av}(t) = MW_{M_1} \cdot \left(\frac{R_{p1}}{R_p}\right) + MW_{M_2} \cdot \left(\frac{R_{p2}}{R_p}\right)$$

The number and weight average molecular weights of the accumulated copolymer are given by

$$\overline{M_n}(t) = \frac{\int_0^t M_{av}(t)R_p(t)V(t)dt}{\int_0^t \left(\frac{M_{av}(t)R_p(t)V(t)}{M_n(t)}\right)dt}$$

$$\overline{M_w}(t) = \frac{\int_0^t M_{av}(t)R_p(t)V(t)M_w(t)dt}{\int_0^t M_{av}(t)R_p(t)V(t)dt}$$

The polydispersity index (PDI) is defined as

$$PDI = \frac{\overline{M_w}(t)}{\overline{M_n}(t)}$$

The instantaneous average composition of the copolymer chain is given by

$$F_i = \frac{R_{pi}}{R_p} \ (i = 1,2)$$

Stockmayer derived the instantaneous bivariate distribution of composition and chain length and found that the chain composition follows a normal distribution with mean F_1. Tacx et al. (1988) generalized Stockmayer's equation when the monomer molecular weights are different and the instantaneous bivariate distribution can be expressed as [7,26,27]

$$W(r,y,t) = \left[1 + \frac{y\left(MW_{M_1} - MW_{M_2}\right)}{F_1 \cdot MW_{M_1} + (1-F_1)\cdot MW_{M_2}}\right](\tau+\beta)\left[\tau + \frac{\beta}{2}(\tau+\beta)(r-1)\right]\cdot r$$
$$\cdot \left(\frac{1}{1+\tau+\beta}\right)^r \frac{1}{\sqrt{2\pi\sigma^2}} exp\left(-\frac{y^2}{2\sigma^2}\right)$$

Where

$$\sigma^2 = F_1(1 - F_1)\frac{\kappa}{r}$$

$$\kappa = [1 - 4F_1(1 - F_1)(1 - r_1 \cdot r_2)]^{0.5}$$

The bivariate distribution of binary copolymer chains accumulated in a batch or semi-batch reactor could be calculated as

$$\bar{W}(r, y, t) = \frac{\int_0^t W(r, y, t) R_p(t) V(t) M_{av}(t) dt}{\int_0^t R_p(t) V(t) M_{av}(t) dt}$$

The instantaneous molecular weight distribution of the copolymer follows

$$W(r, t) = (\tau + \beta)\left[\tau + \frac{\beta}{2}(\tau + \beta)(r - 1)\right] \cdot r \cdot \left(\frac{1}{1 + \tau + \beta}\right)^r$$

The accumulated molecular weight can be determined by the integration over time of the above equation

$$\bar{W}(r, t) = \frac{\int_0^t W(r, t) R_p(t) V(t) M_{av}(t) dt}{\int_0^t R_p(t) V(t) M_{av}(t) dt}$$

The kinetic expressions follow the Arrhenius law; a summary of the different rate constant relations and some physical component properties used in the model are presented in the following table.

	Rate expression	**Ref.**
Initiation	$k_d(s^{-1}) = 9.24\text{x}10^4 e^{\left(\frac{-14915}{T}\right)}$ Factor efficiency = 0.8 ($f = 0.8$)	[28]

Propagation	$k_{p11}\left(\frac{L}{mol \cdot s}\right) = 9.5\text{x}10^{7} e^{\left(\frac{-2189}{T}\right)} e^{[-w_{N_1}(0.0016 \cdot T + 1.015)]}$ $k_{p22}\left(\frac{L}{mol \cdot s}\right) = 3.2\text{x}10^{7} e^{\left(\frac{-1564}{T}\right)} [0.11 + 0.89 e^{-3 w_{N_2}}]$	[29] [28]
Termination	$k_{t11}\left(\frac{L}{mol \cdot s}\right) = 2\text{x}10^{10} e^{\left(-\frac{1991 + 1477 w_{N_{1,0}}}{T}\right)}$ $k_{t22}\left(\frac{L}{mol \cdot s}\right) = 9.8\text{x}10^{11} e^{\left(-\frac{1860}{T}\right)} \left(1.56 - 1.77 w_{N_{2,0}} - 1.2 w_{N_{2,0}}\right) 30^{-0.44} (10^{4.5})^{-0.16}$ $k_{t21} = k_{t12} = \frac{k_{t11} + k_{t22}}{2}$	[29] [28]
Transfer to monomer	$k_{f11}\left(\frac{L}{mol \cdot s}\right) = k_{f12} = k_{p11} \cdot 0.00118 e^{\left(-\frac{1002}{T}\right)}$ $k_{f22}\left(\frac{L}{mol \cdot s}\right) = k_{f21} = k_{p22} \cdot 7.5\text{x}10^{-5}$	[29] [28]
Densities	$\rho_{M_1}\left(\frac{g}{L}\right) = (1.048 - 3\text{x}10^{-3} T - 6\text{x}10^{-6} T^2)$ $\rho_{M_2}\left(\frac{g}{L}\right) = (1.073 - 1.0826\text{x}10^{-3} T - 7.2379\text{x}10^{-7} T^2)$ $\rho_{S}\left(\frac{g}{L}\right) = (0.9999 + 2.3109\text{x}10^{-5} T - 5.44807\text{x}10^{-6} T^2)$	[29] [28] [28]
Molecular weights	$MW_{M_1}\left(\frac{kg}{kmol}\right) = 71.08$ $MW_{M_2}\left(\frac{kg}{kmol}\right) = 72.06$ $MW_{I}\left(\frac{kg}{kmol}\right) = 271.19$ $MW_{S}\left(\frac{kg}{kmol}\right) = 18.01$	
Heat of polymerization	$\Delta H_{p1}\left(\frac{kJ}{kmol}\right) = 82.2\text{x}10^{3}$	[30]

	$\Delta H_{p2}\left(\frac{kJ}{kmol}\right) = 79.2\text{x}10^3$	[31]
Reactivity Ratios	$r_1 = (0.491 + 1.442\alpha) + (0.006 - 1.362\alpha)w_{N_{1,0}}$ $r_2 = (1.287 - 1.105\alpha) + (-0.107 + 1.207\alpha)w_{N_{2,0}}$ $\alpha = 0.5$ (ionic strength)	[18] [18]

As we mentioned in the first section, we are estimating the copolymer microstructure for different reactor configurations (batch and semi-batch). We may understand and predict how different conditions will affect, for example, the cumulative monomer composition or the average molecular weight at final conversion. The simulation for each reactor and thermal condition (isothermal and adiabatic) requires solving a system of 9 nonlinear ordinary differential equations. Then, the data was collected and reprocessed to estimate the copolymer properties of interest. All the simulations and data analysis were done with MATLAB®.

4. Results

In this section, the simulations and results for the different cases are presented. First, the studies for the batch reactor with isothermal and non-isothermal conditions are shown. Second, two simulations for a semi-batch reactor with isothermal and non-isothermal configurations are analyzed. Third, we simulated the response for the isothermal semi-batch reactor with the necessary inflow feed as a function of time that produces a desired copolymer where the acrylamide inflow was disturbed with white noise. Different standard deviations for the white noise were selected to compare how the copolymer microstructures vary at the end of monomer conversion. This was done to simulate a possible industrial situation where the flows are not

exactly constant or equal to the setpoint which are naturally caused by random disturbances. Finally, because the noise may play a significant role in the final microstructure, the implementation of a PD controller aiming to control the reactor temperature in the semi-batch isothermal scenario has been tuned.

4.1. Part I

Batch Reactor – Isothermal Conditions (Case I)

The initial conditions for this configuration are presented in Table I.

Variable	
Initial fraction of acrylamide in the reactor	$f_{AAm,0} = 0.7$
Total monomer concentration	$w_{M,0} = 15\ wt\%$
Reactor temperature	$T = 50℃$
Initiator concentration	$[I]_0 = 0.001M$

Table I – Initial conditions for the isothermal batch reaction.

Figure I to Figure VII depict the simulation results for the isothermal batch reactor.

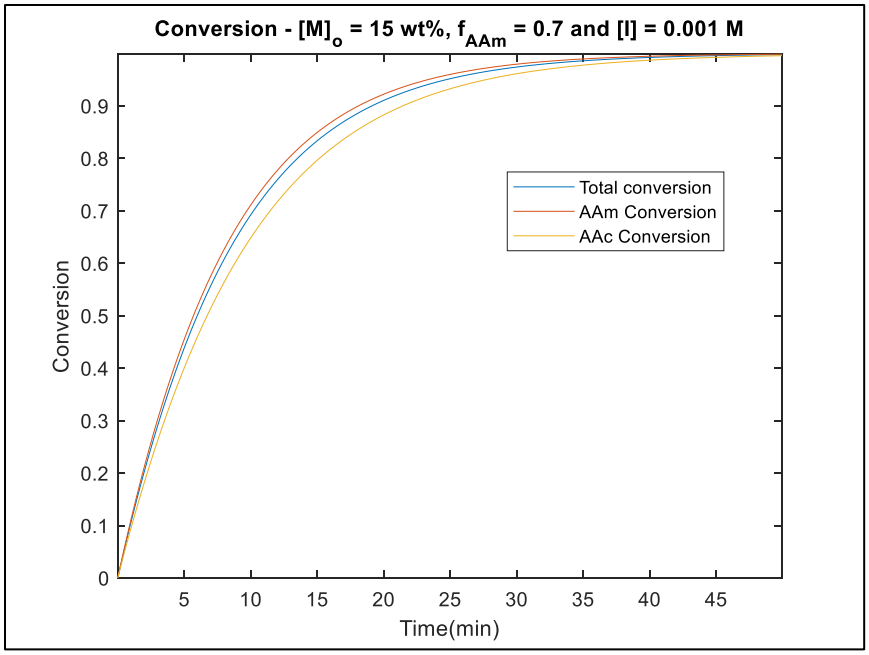

Figure I – Monomer (total and individual) conversions as a function of time for isothermal operation. AAm and AAc have similar reactivity ratios but for AAm is slightly higher which makes it more reactive and for that reason is consumed faster than AAc. This will cause composition drift in the copolymer especially in the absence of AAm.

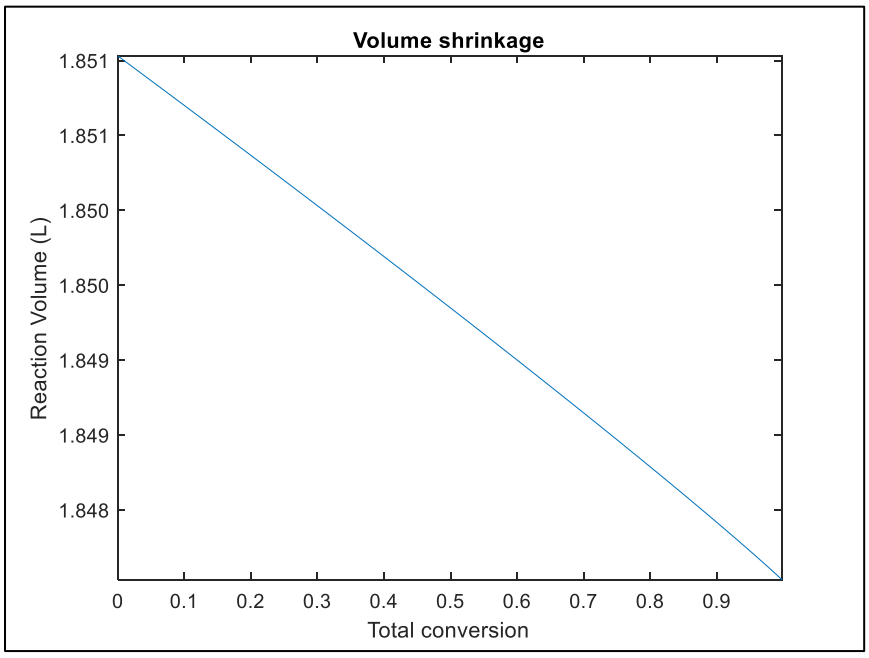

Figure II – Volume variation as function of the total monomer conversion. The reaction volume is reduced as the reaction advance due to the copolymer density but there is not a significant change.

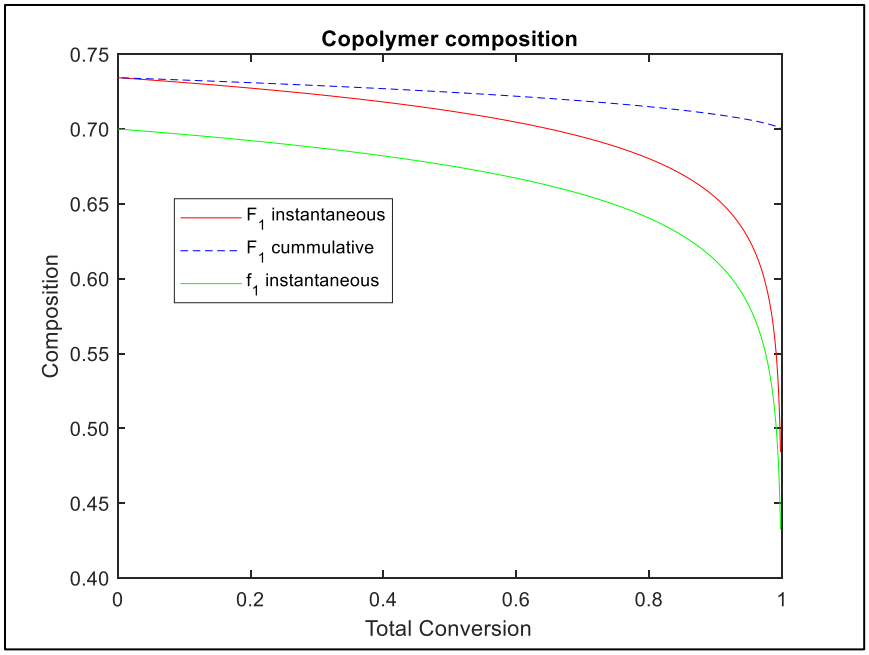

Figure III – Red line: Instantaneous AAm composition in the copolymer, Green line: AAm fraction in the reactor mixture, Blue doted line: Cumulative AAm composition in the copolymer. The instantaneous AAm composition refers to the AAm monomers being added to the copolymer at specific conversion. At higher conversions, this composition decreases because there is no more AAm in the mixture and practically only AAc is being added to the copolymer. However, the cumulative AAm composition at the end of the reaction is 70 %.

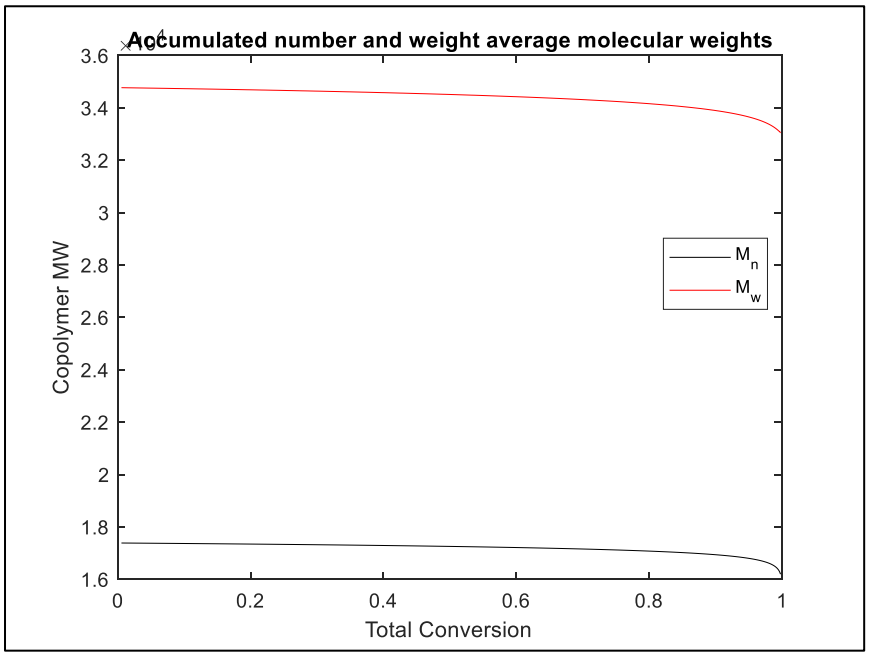

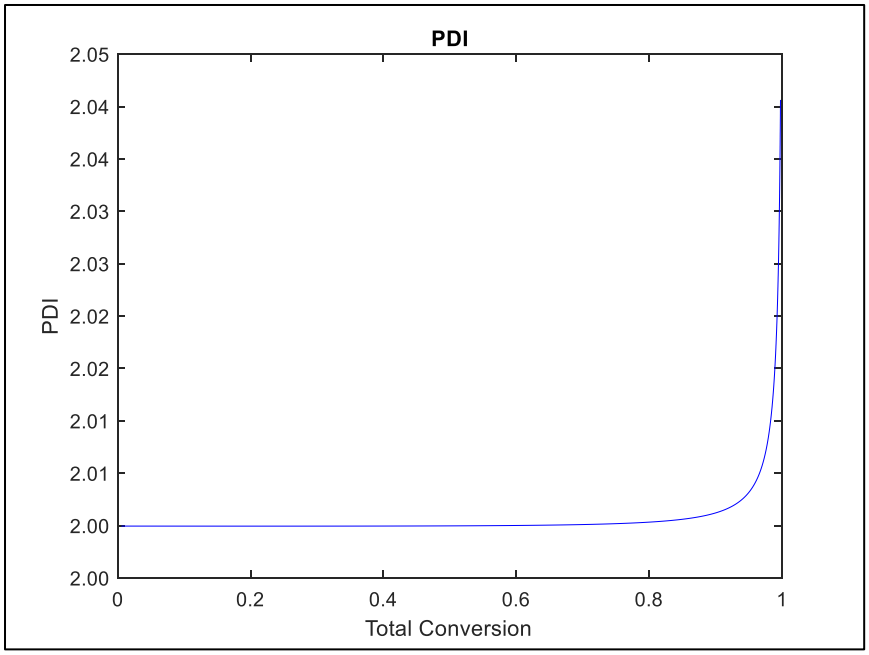

Figure IV and Figure V – Top: It is presented the variation with total monomer conversion of the number and weight average molecular weights. Because it is isothermal process, we do not observe considerable changes in its value and are kept constant almost for all conversion values. Bottom: The polydispersity index as function of total monomer conversion is depicted. There is no significant variation in its value throughout the reaction and it keeps constant in 2.

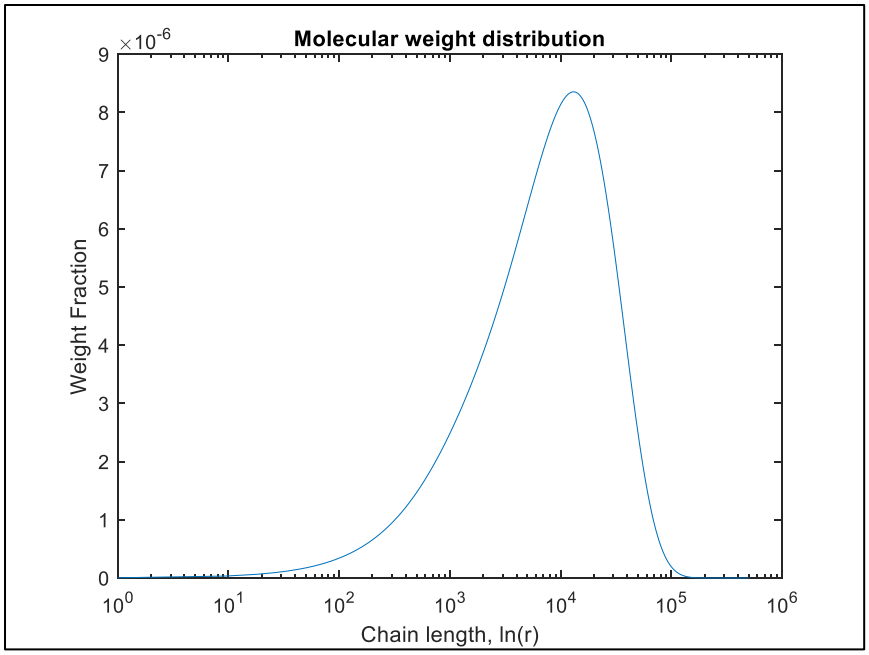

Figure VI – Cumulative molecular weight distribution of the copolymer at full conversion for isothermal conditions.

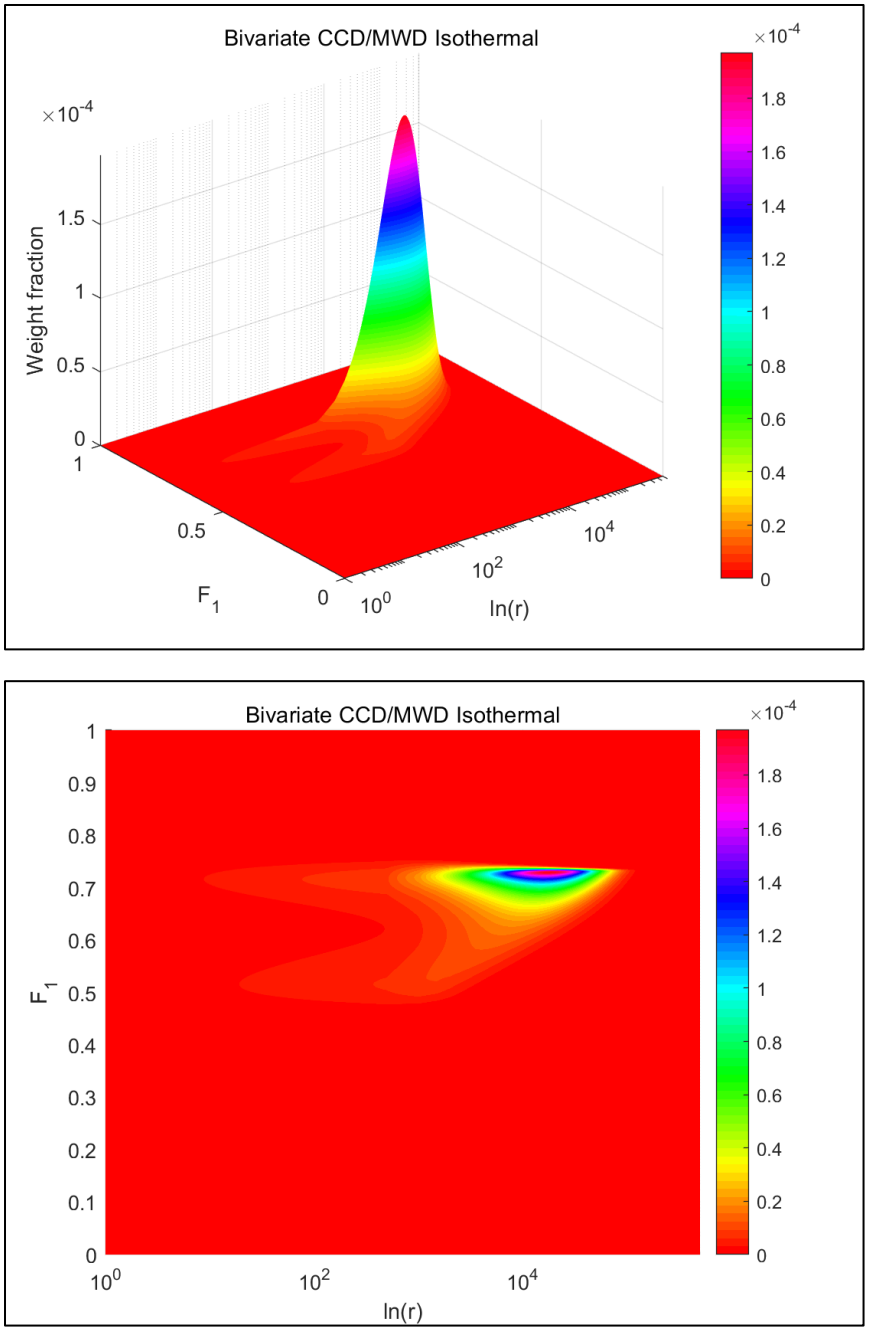

Figure VII and Figure VIII – Bivariate chemical composition/molecular weight distribution of the copolymer at full conversion. We can observe a very good narrow distribution for the copolymer microstructure.

Batch Reactor – Non-Isothermal Conditions (Case II)

The initial conditions for this configuration are presented in Table II.

Variable	
Initial fraction of acrylamide in the reactor	$f_{AAm,0} = 0.7$
Total monomer concentration	$w_{M,0} = 15\ wt\%$
Initial reactor temperature	$T_0 = 20°C$
Initial initiator concentration	$[I]_0 = 0.001M$

Table II – Initial conditions for the non-isothermal batch reaction. The initial temperature is lower in this case than for the Case I because we are considering the heat reaction of the propagation reactions and the temperature will increase faster.

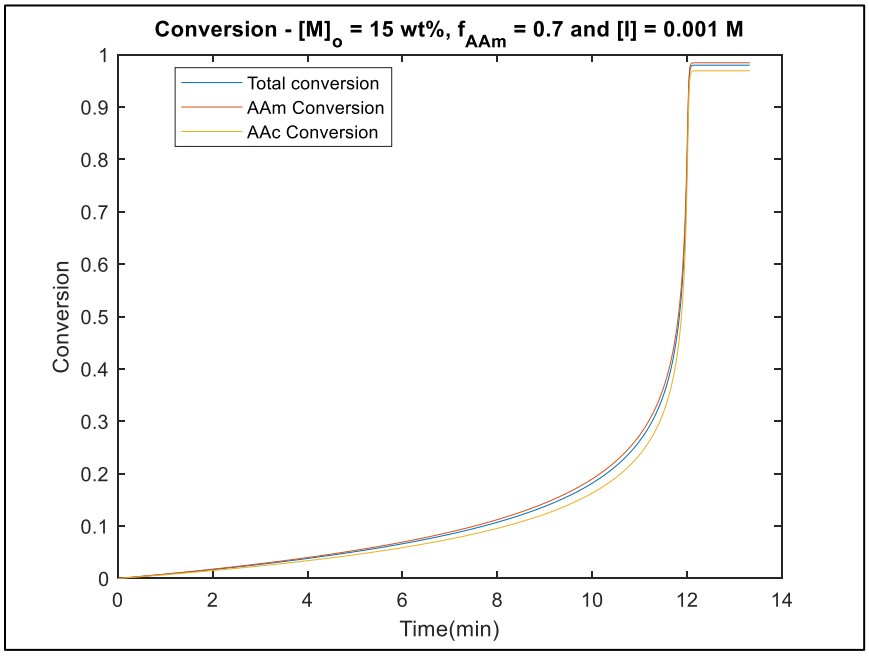

Figure IX - – Monomer (total and individual) conversions as a function of time for non-isothermal operation. As we can observe, the time required to complete the reaction is smaller than isothermal reaction. That is basically for the significant reaction heat for each of the propagation reactions. For this case, the conversion is not complete, and this is due to very high reaction temperature leads to greater kinetic constants and when the conversion is close to one there is no more initiator in the reactor mixture and the process stopped.

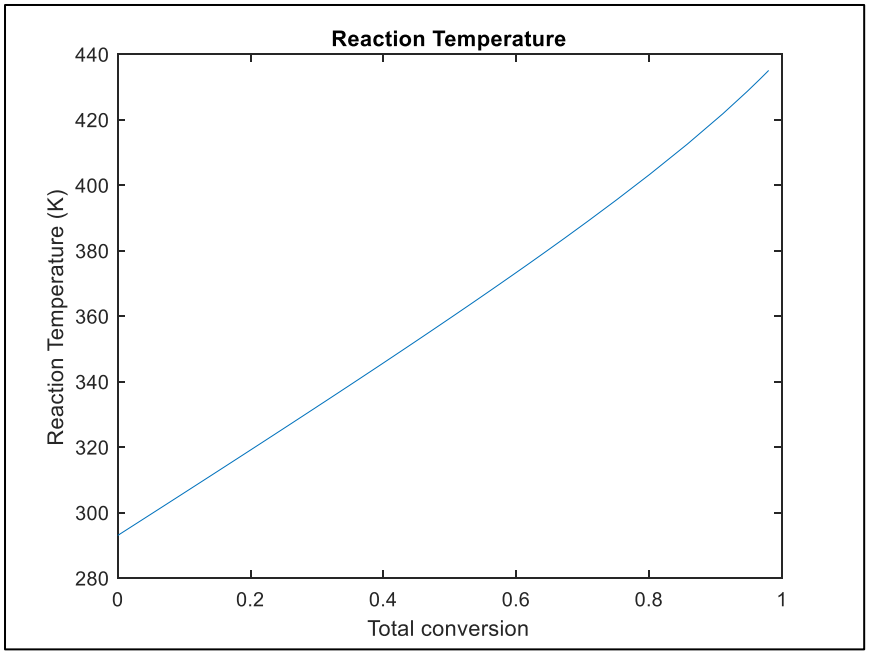

Figure X – Temperature reaction as a function of the total monomer conversion in non-isothermal conditions. The temperature variation with conversion is almost a perfect line and the final temperature in the reactor is 160 ˚C.

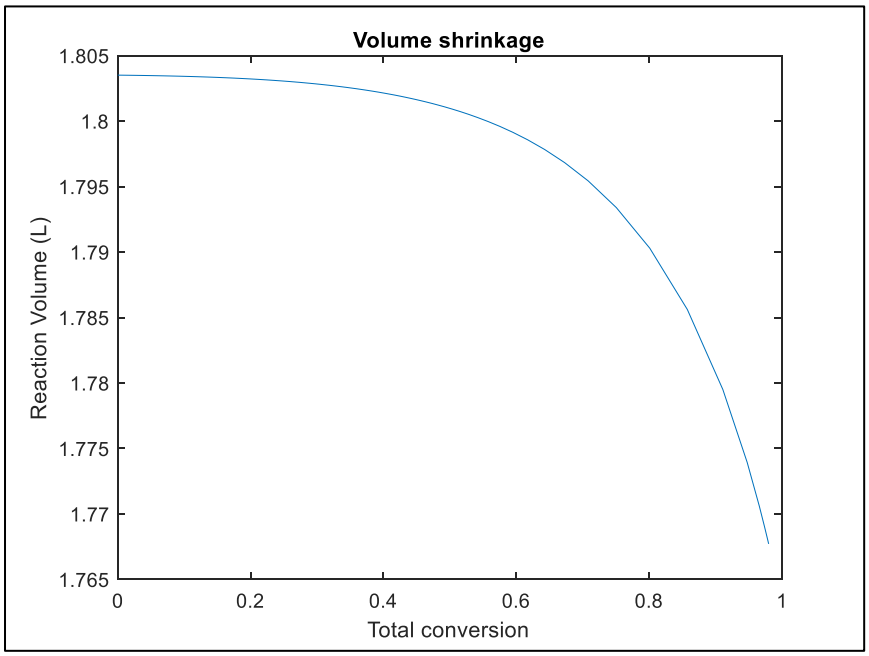

Figure XI – Volume reaction variation as a function of the total monomer conversion. For this case, the variation is not linear because the density of the components (monomers, solvent and polymer) are changing as the reaction temperature changes.

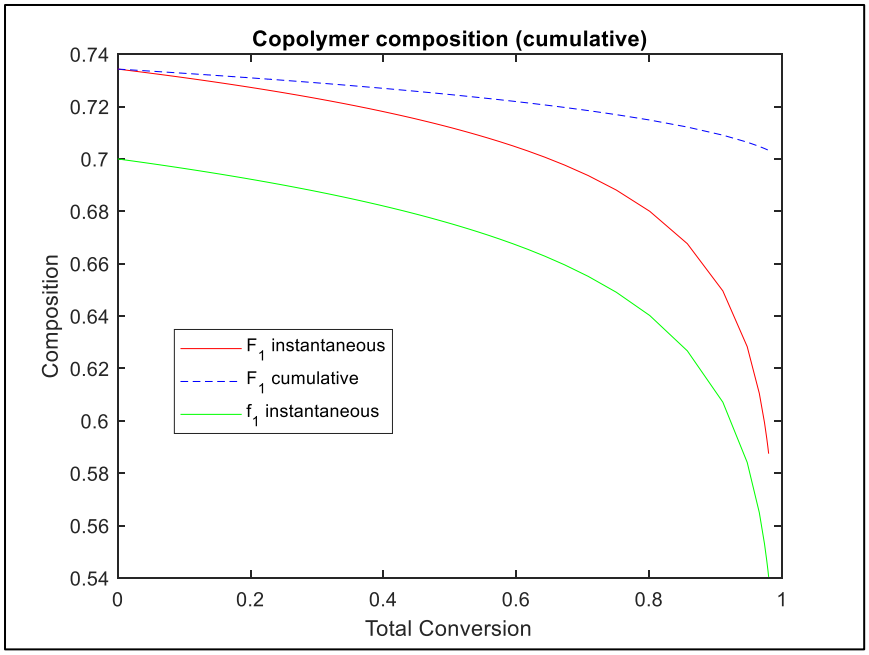

Figure XII – Copolymer cumulative composition. There is not great variation in the final copolymer composition because the reactivity ratios depend on the initial concentration of the monomers and in the ionic strength which have kept them unchanged in both simulations.

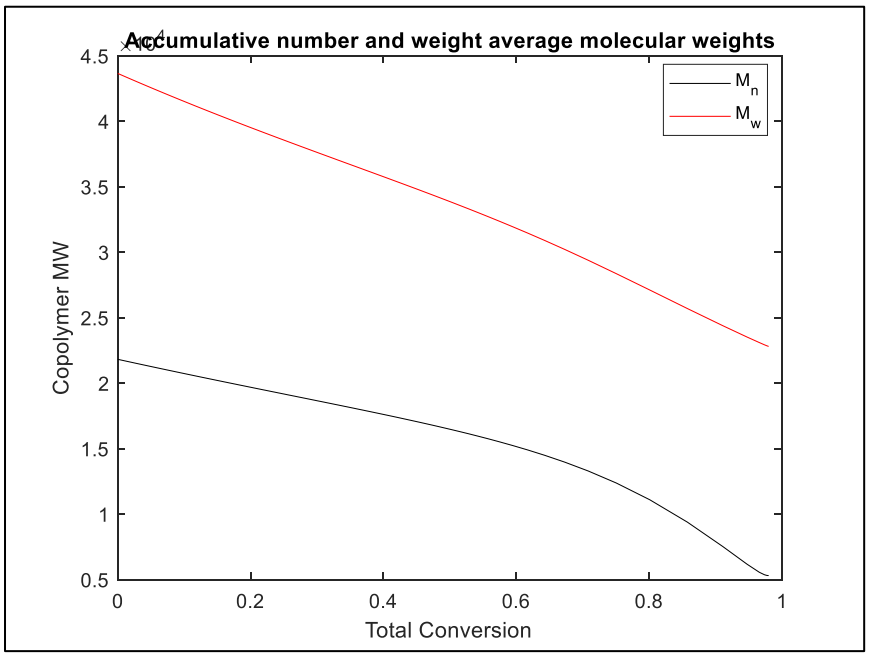

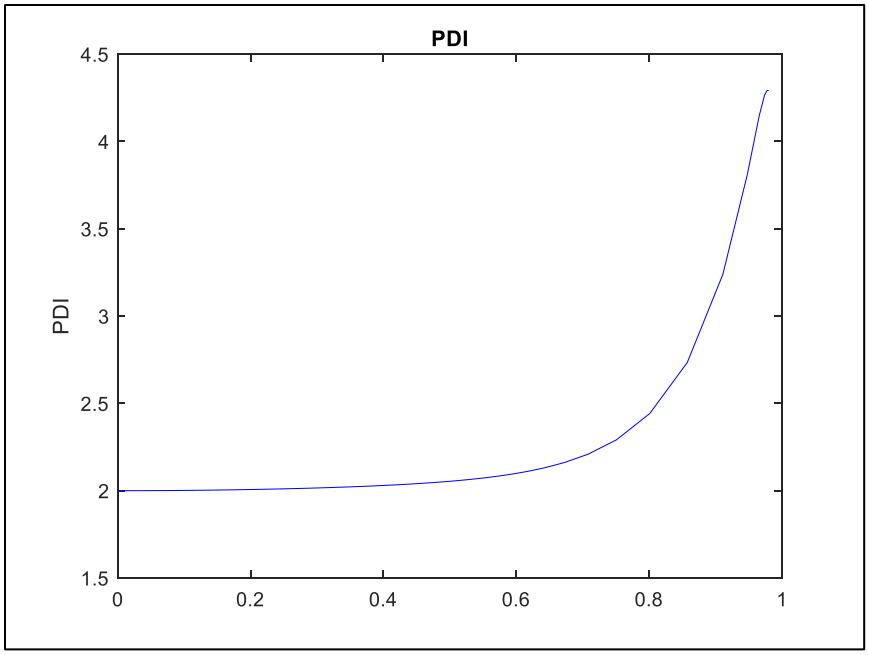

Figure XIII and Figure XIV – Top: Accumulative number and weight average molecular weight as a function of the total monomer conversion. In this case, the values of both parameters decrease as the reaction advance, which is consistent with the inverse proportional relation that they have with the reaction temperature. Bottom: Polydispersity index as a function of total monomer conversion. At the end of the reaction, the PDI increases to over 4, where the abrupted decrease in the number molecular weight leads to an increase in the PDI value.

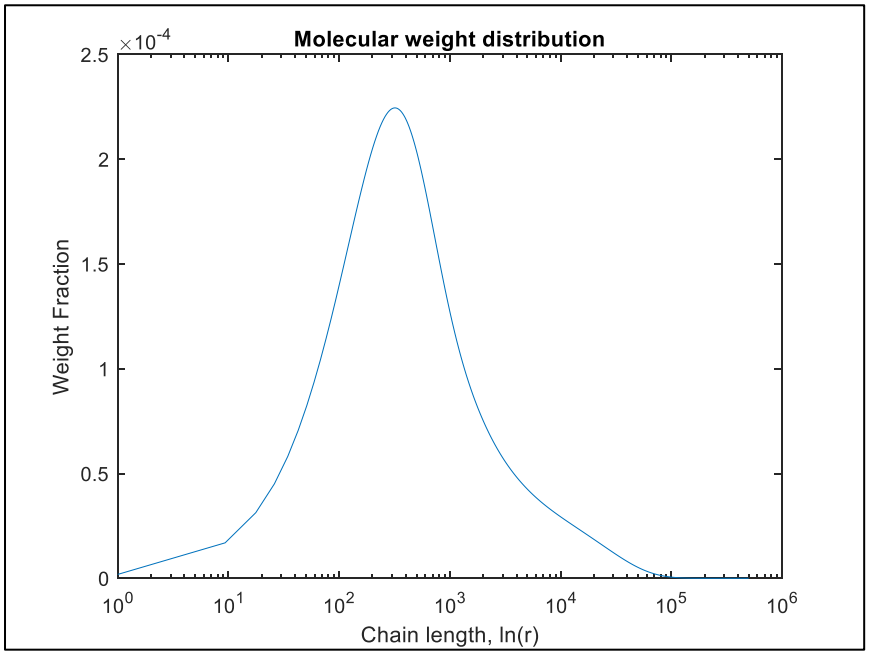

Figure XV - Cumulative molecular weight distribution of the copolymer at full conversion for non-isothermal conditions. There is a decrease in the average chain length because of the temperature variation. A higher temperature indicates higher kinetic rate constants, so the undesired reactions such as transfer to monomer or termination occur when the chain length is not as long as the isothermal case.

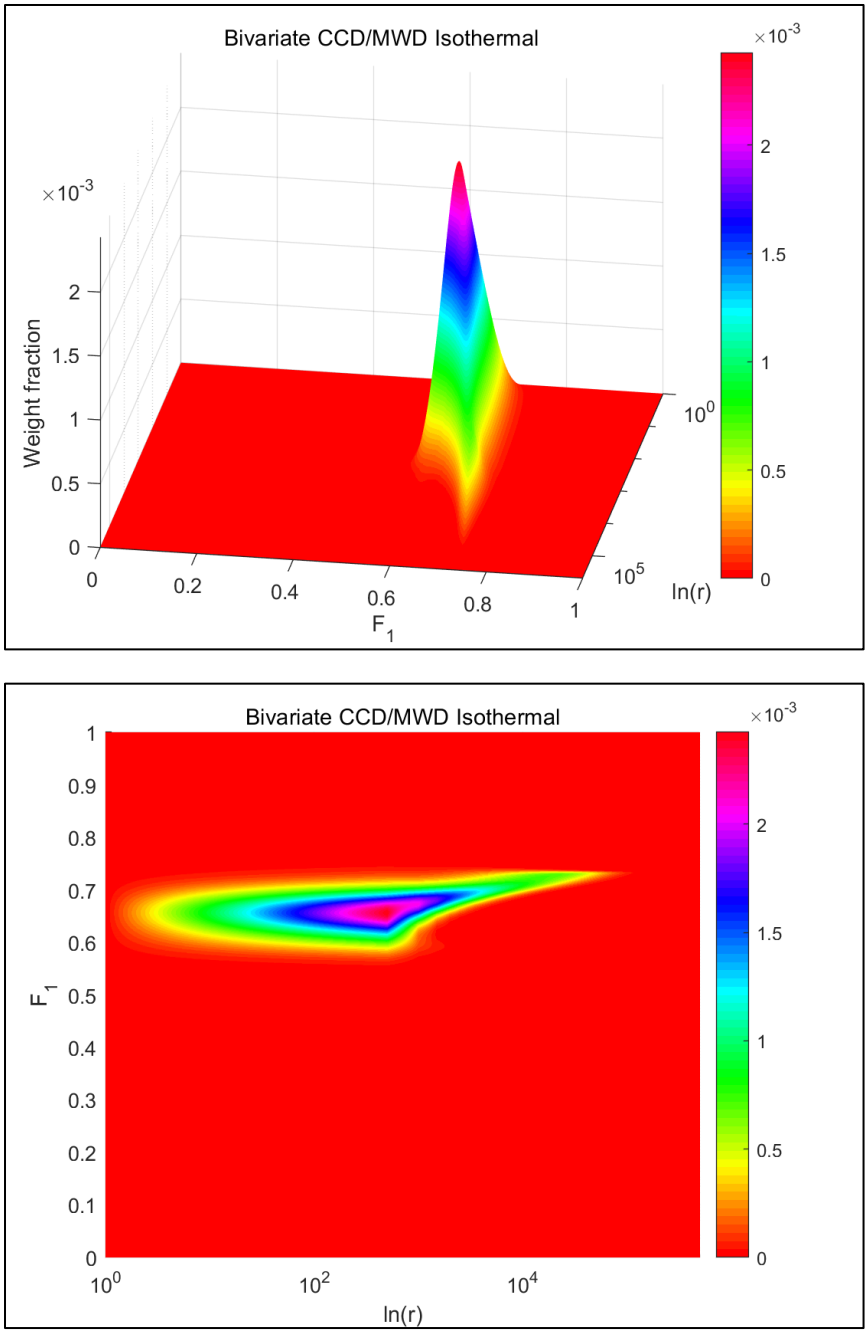

Figure XVI and Figure XVII - Bivariate chemical composition/molecular weight distribution of the copolymer at full conversion. We can observe that in this case the average molecular weight is shifted to a small value because of the variation temperature. Although we are not getting a nice narrow distribution among the chain length, the variation in the copolymer composition for the different chain lengths at the end of reaction are similar and close to the desired value of acrylamide copolymer composition of 0.7.

4.2. Part II

Semi-Batch Reactor – Isothermal Conditions (Case III)

The initial conditions for this configuration are presented in Table III.

Variable	
Initial fraction of acrylamide in the reactor	$f_{AAm,0} = 0.7$
Total monomer concentration	$w_{M,0} = 15\ wt\%$
Reactor temperature	$T = 50℃$
Initial initiator concentration	$[I]_0 = 0.001M$

Table III – Initial conditions for the isothermal semi-batch simulation.

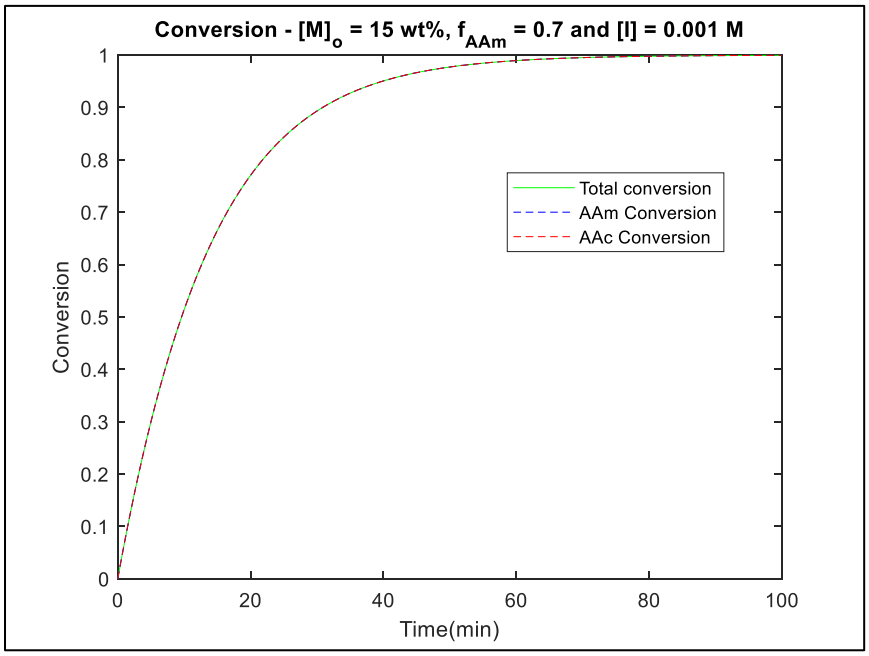

Figure XVIII - Monomer (total and individual) conversions as a function of time for isothermal operation in a semi-batch reactor configuration. As we can observe, the time required to complete the reaction is greater than the isothermal batch reaction (same reaction temperature of 50 ˚C). This is because we are constantly adding acrylamide monomer to keep the initial monomer relation in the mixture constant throughout the complete reaction. There is almost no difference between the individual and total conversion due to the monomer relation in the reaction mixture is keeping constant.

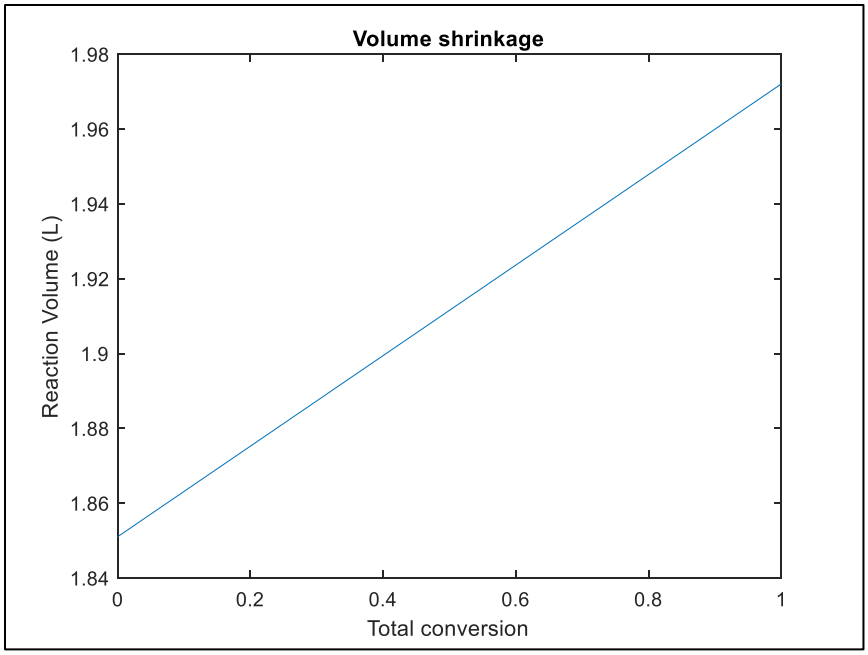

Figure XIX – Volume reaction as a function of the total monomer conversion. In this case, the variation is linear, and the volume is increasing due to the constant addition into the reactor of acrylamide moles.

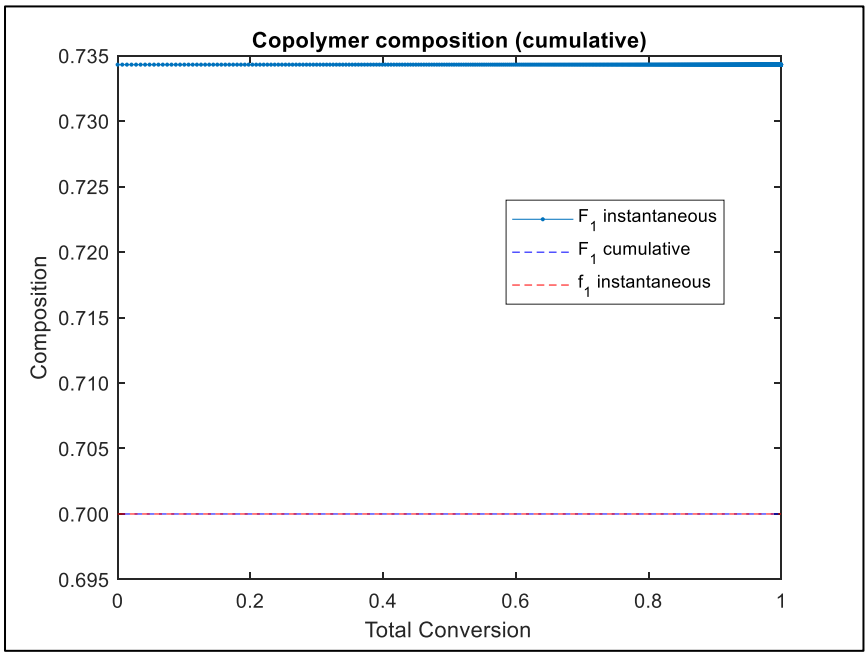

Figure XX - Copolymer cumulative composition in a semi-batch isothermal reactor. As we may expect in this situation with this policy, the cumulative copolymer composition is constant through all the reaction due to the addition of acrylamide to keep the same monomer mixture relation all the time.

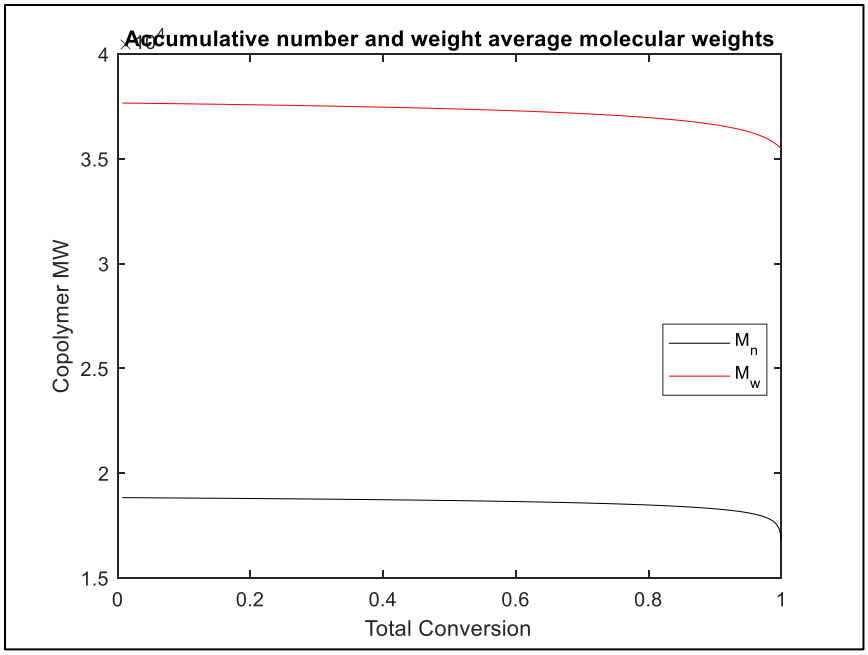

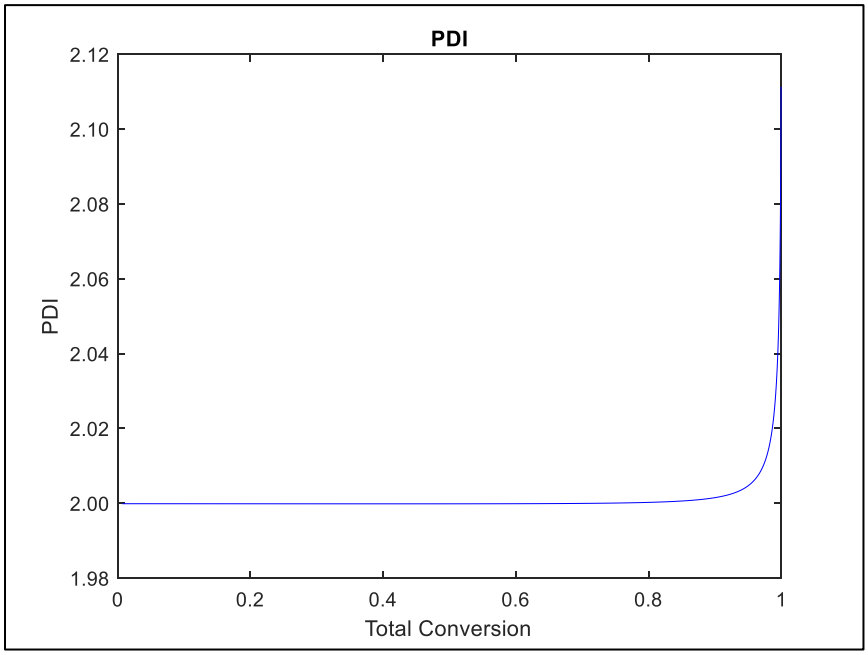

Figure XXI and Figure XXII - Top: Accumulative number and weight average molecular weight as a function of the total monomer conversion. For this case, the values of both parameters are almost constant as the reaction advances, which is consistent with a constant temperature reaction. Bottom: Polydispersity index as a function of total monomer conversion. At the end of the reaction, the PDI increases but stayed constant for the major part of the reaction.

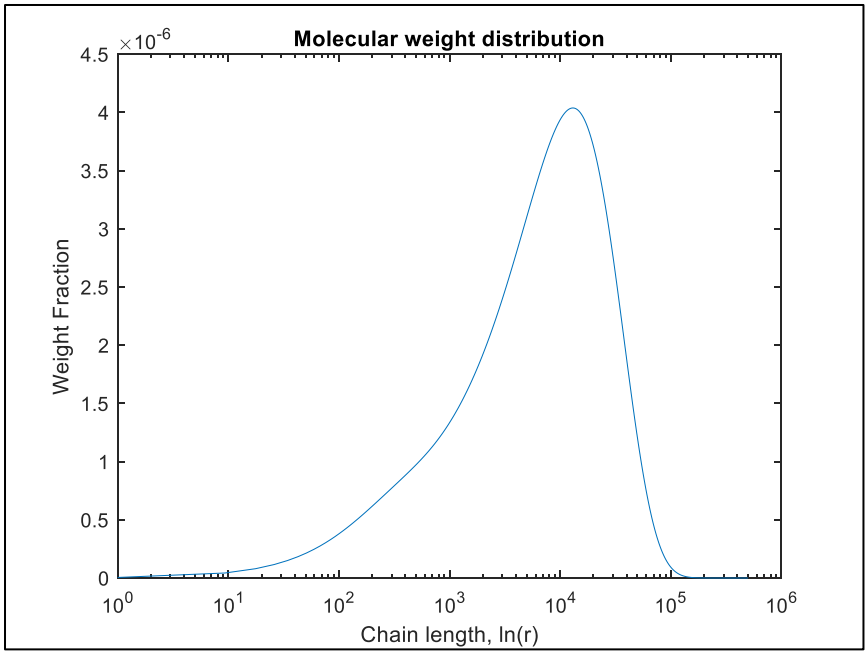

Figure XXIII - Cumulative molecular weight distribution of the copolymer at full conversion for semi-batch isothermal conditions. Although the average chain length is practically the same as the isothermal batch reactor, we may observe a major presence of shorter chains between 10^2 to 10^3. This may be linked with the unchanged monomer concentration relation in the mixture during the reaction that conduct to keep the propagation rate constant ratio constant and then to smaller chain lengths.

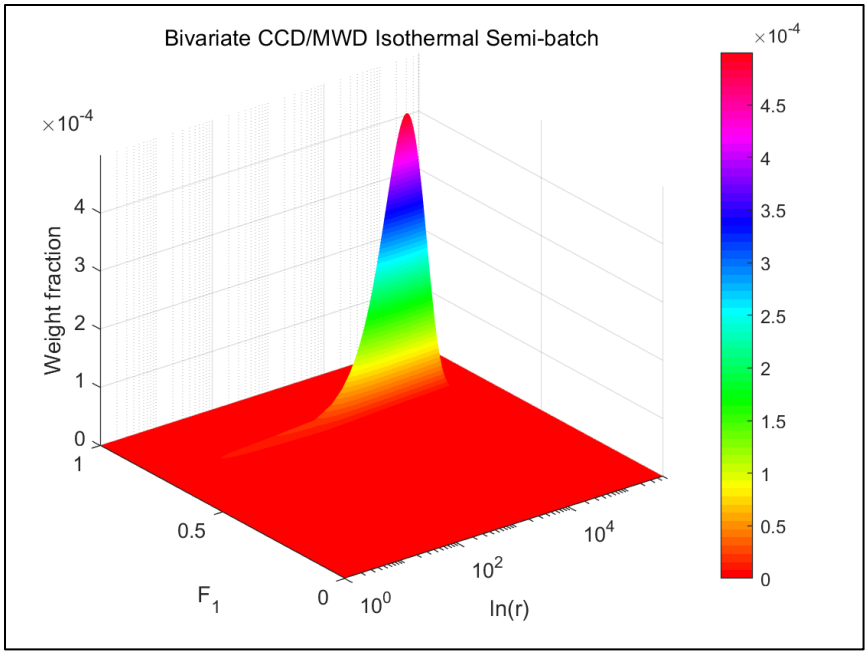

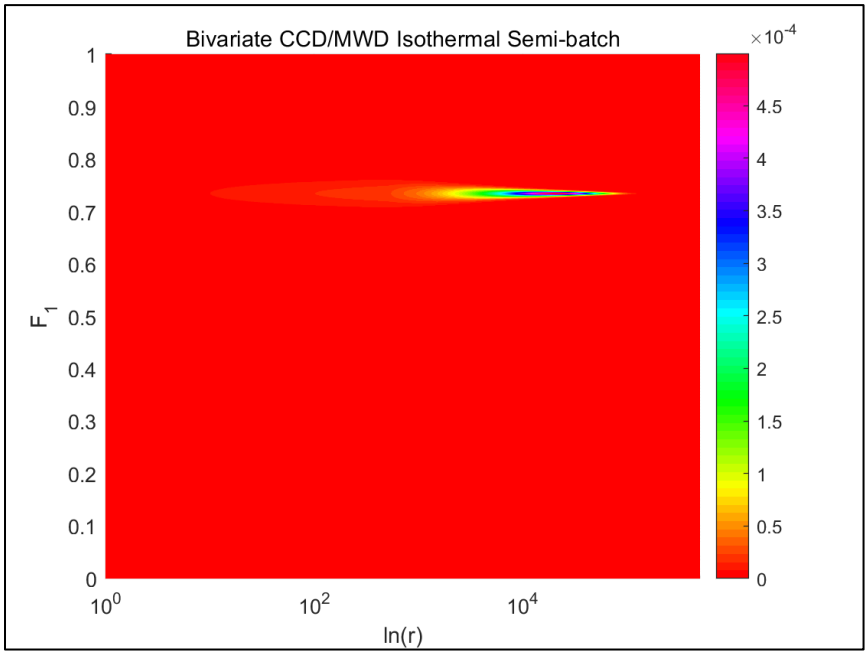

Figure XXIV and Figure XXV - Bivariate chemical composition/molecular weight distribution of the copolymer at full conversion. We can observe that although the average molecular weight is 10^4, it is inevitable to avoid the copolymer chain formation with smaller lengths. Nonetheless, the copolymer composition for all the different chains have a very narrow distribution over 0.7 due to the constant monomer mixture relation within the reactor at every time.

Semi-Batch Reactor – Non-isothermal Conditions (Case IV)

The initial conditions for this configuration are presented in Table IV.

Variable	
Initial fraction of acrylamide in the reactor	$f_{AAm,0} = 0.7$
Total monomer concentration	$w_{M,0} = 15\ wt\%$
Initial reactor temperature	$T = 20\ ℃$
Initial initiator concentration	$[I]_0 = 0.001\ M$
Temperature of acrylamide mole inflow	$T_{F_{N_{1,i}}} = 20\ ℃$

Table IV – Initial conditions for the non-isothermal semi-batch simulation.

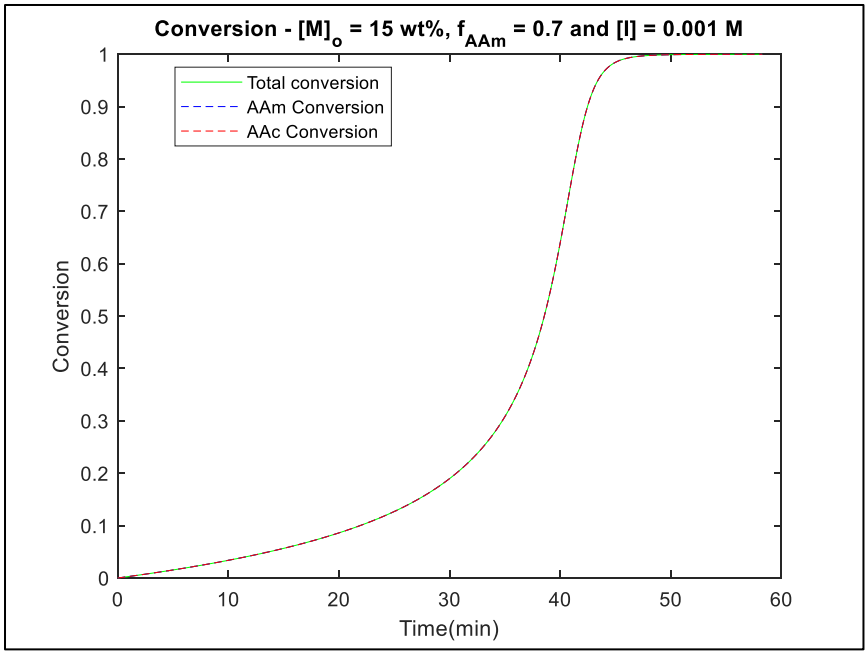

Figure XXVI - Monomer (total and individual) conversions as a function of time for non-isothermal operation in a semi-batch reactor configuration. As we can observe, the time required to complete the reaction is lower than the isothermal semi-batch reaction, but it is greater than the non-isothermal batch reactor. This is because we are constantly adding acrylamide monomer to keep the initial monomer relation in the reaction mixture constant, and because it was at 20 °C the reaction temperature did not rise as fast as the Case II and then the reaction time is longer. There is almost no difference between the individual and total conversion due to the monomer relation in the reaction mixture is always constant.

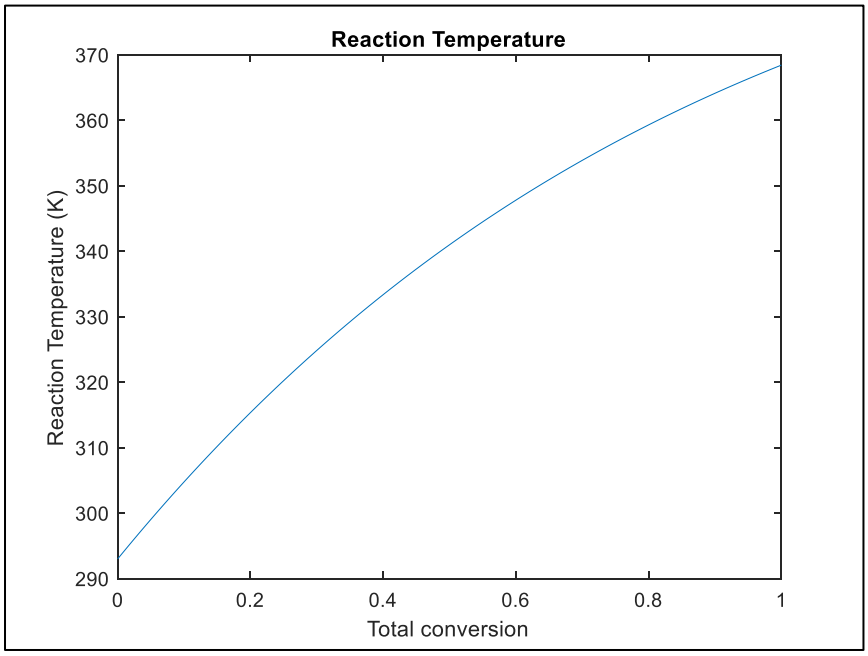

Figure XXVII - Temperature reaction as a function of the total monomer conversion for Case IV. The temperature variation with conversion is not linear and the maximum temperature at the end of reaction is almost 100 °C. That is because the monomer inflow is at 20 °C which helps to refrigerate the reaction mixture.

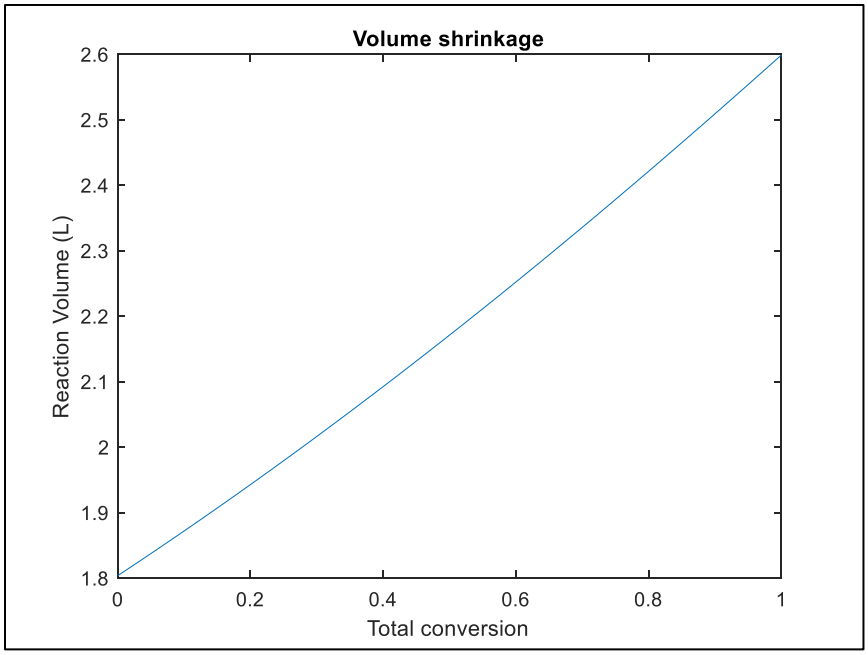

Figure XXVIII - Volume reaction as a function of the total monomer conversion. In this case, the final volume is greater than the Case III because the lower mixture temperature during the whole reaction entails to add more acrylamide moles to keep the relation constant.

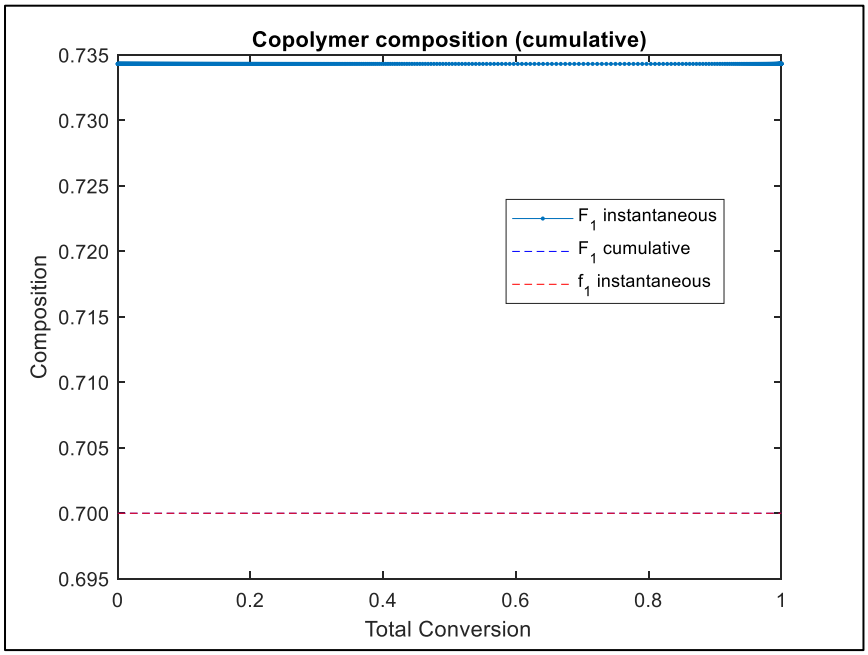

Figure XXIX - Copolymer cumulative composition in a semi-batch non-isothermal reactor. As we may expect in this situation with this policy, the cumulative copolymer composition is constant through all the reaction due to the addition of acrylamide to keep the same monomer mixture relation every time.

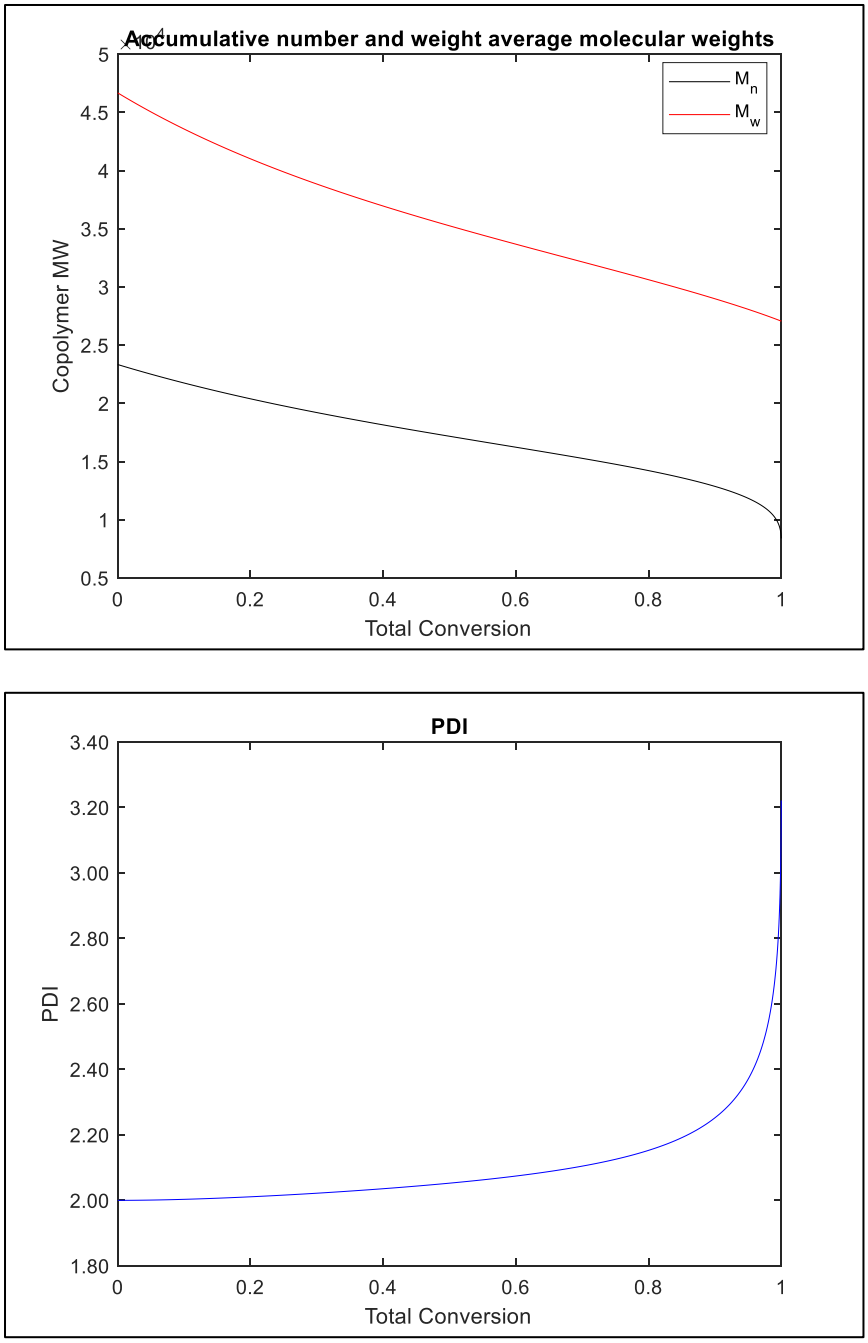

Figure XXX and Figure XXXI - Top: Accumulative number and weight average molecular weight as a function of the total monomer conversion. For this case, the values of both parameters are decreasing as the reaction advances, which is consistent because of the inverse relation with the temperature. Bottom: Polydispersity index as a function of total monomer conversion. At the end of the reaction, the PDI increases but not as much as the Case II due to lower temperature.

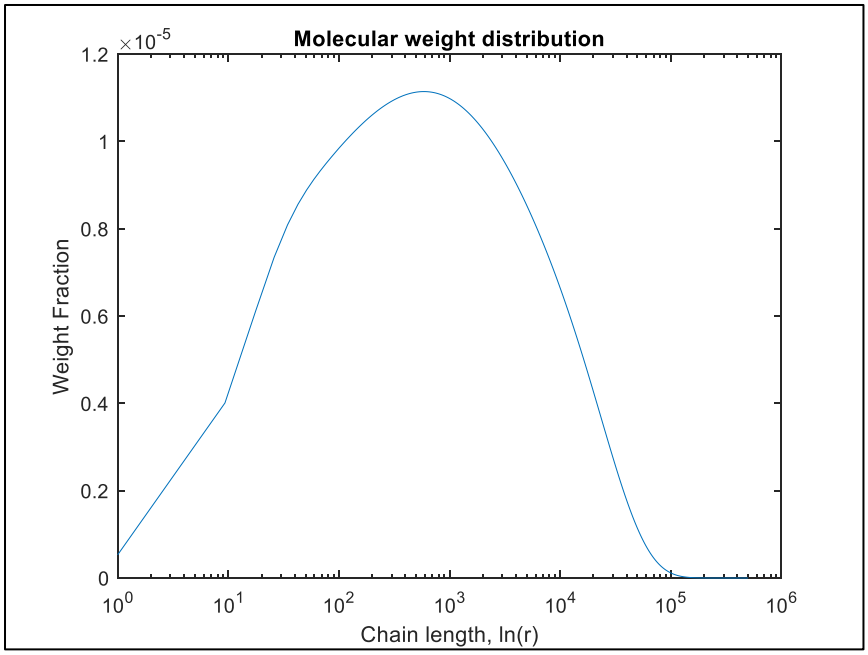

Figure XXXII - Cumulative molecular weight distribution of the copolymer at full conversion for semi-batch non-isothermal conditions. Although the average chain length is smaller the isothermal batch reactor, a much broader distribution could be observed. Both, unchanged monomer relation concentration and temperature variation during the reaction time, lead to a wider molecular length distribution.

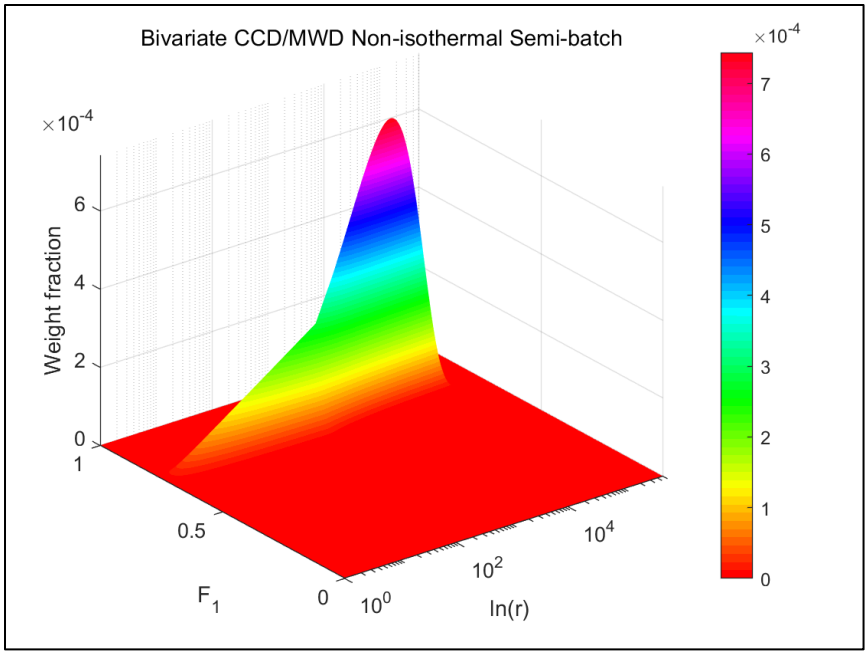

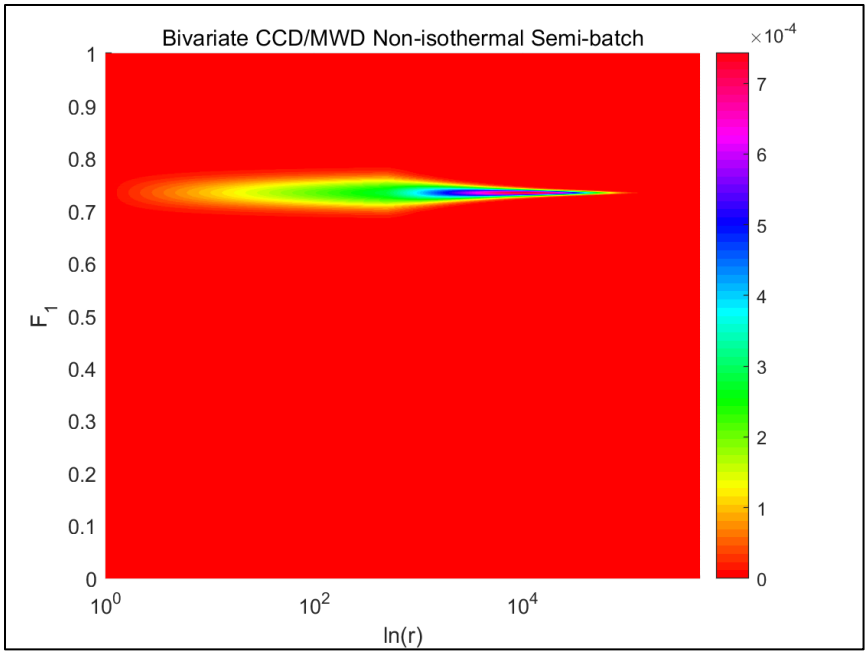

Figure XXXIII and Figure XXXIV - Bivariate chemical composition/molecular weight distribution of the copolymer at full conversion. We can observe that although the average molecular weight is between 10^2 and 10^3, it is inevitable to avoid the copolymer chain formation with smaller lengths. Whereas the copolymer composition for long chains have a very narrow distribution, it gets broader for short chains.

4.3. Part III

Semi-Batch Reactor – Isothermal Conditions with disturbances

Since disturbances in a process are inevitable, we conducted three new simulations for Case III but considering that acrylamide inflow was affected by white noise. To compare the different results, firstly we calculated the necessary acrylamide inflow relation as a function of time to produce the copolymer of Case III, namely the ideal inflow. Secondly, white noise was incorporated into the ideal monomer inflow to simulate the presence of disturbances in the system. Three white noise signals with different standard deviations were tested to analyze how much this change affects the results. Therefore, three new simulations with that noisy inflow were conducted, and the copolymer microstructure for each of them was obtained. From Figure

XXXV to Figure XXXVII, the white noise and the ideal acrylamide inflow are depicted, showing the differences between the ideal and nonideal inflows.

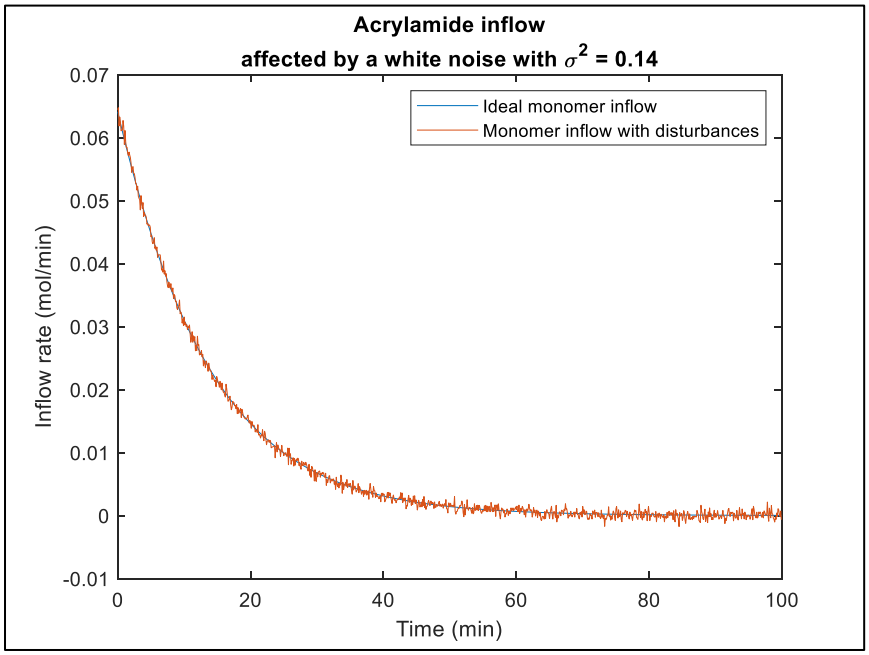

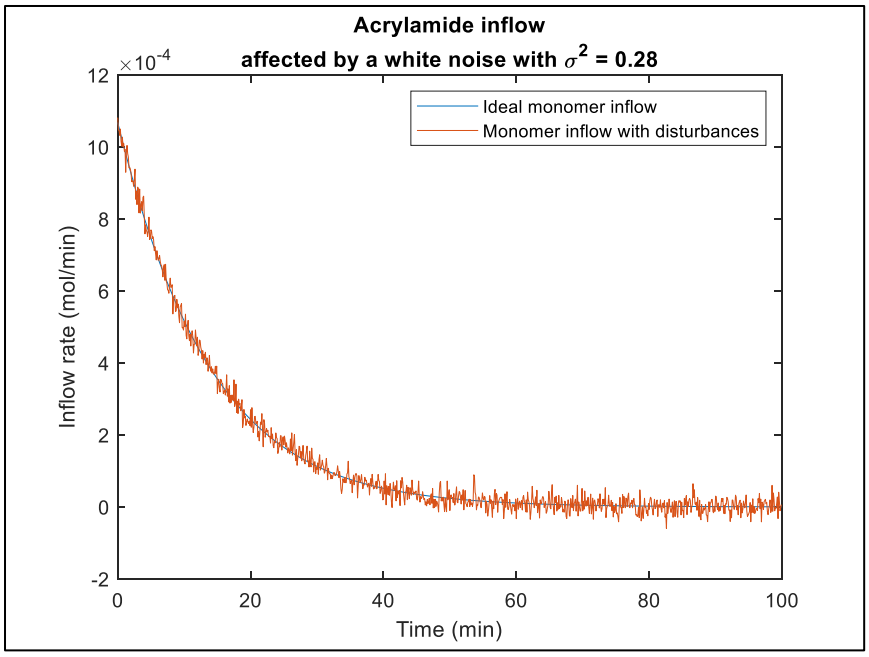

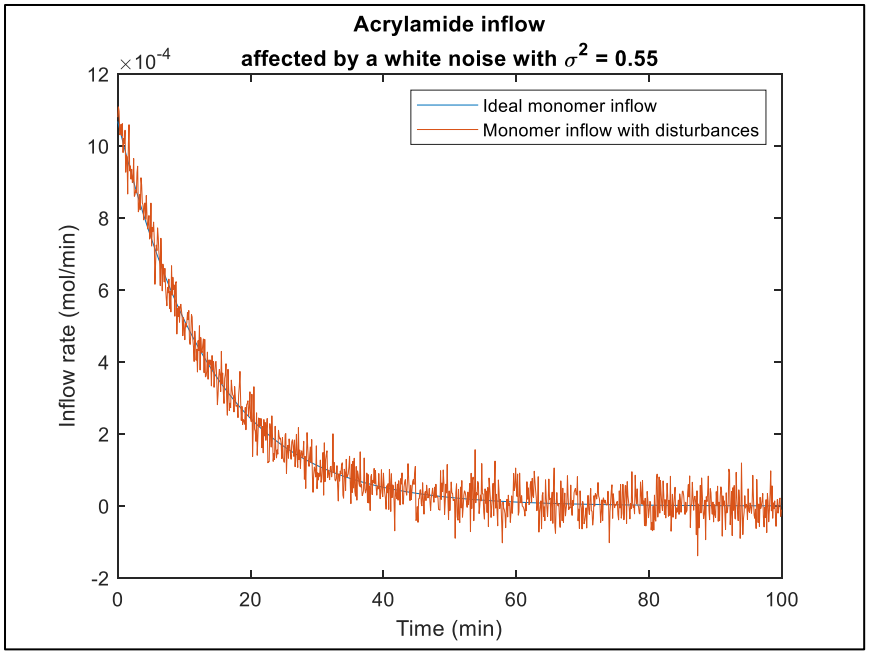

Figure XXXV, Figure XXXVI and Figure XXXVII – From the top to the bottom figure, a graph depicting the presence of disturbances in the monomer inflow are showed. To the first, the standard deviation of the white noise is minor, and a very small deviation of the ideal flow is obtained for every time. Then we increased the standard deviation to get a wider distribution of values around the ideal flow. Finally, the last simulation could be interpreted as an exaggeration of disturbances in the process because the standard deviation is too large for this process and for some specific times, the real inflow is totally apart from the ideal flow.

To simplify and specifically show the variations due to the presence of white noise, only the copolymer composition as a function of time, the bivariate copolymer composition and the accumulated molecular weight distribution at full conversion for each of the different input profiles are presented. We named Case V, VI and VII the results obtained when the standard deviation of the white noise was 0.14, 0.28 and 0.55 respectively.

Case V

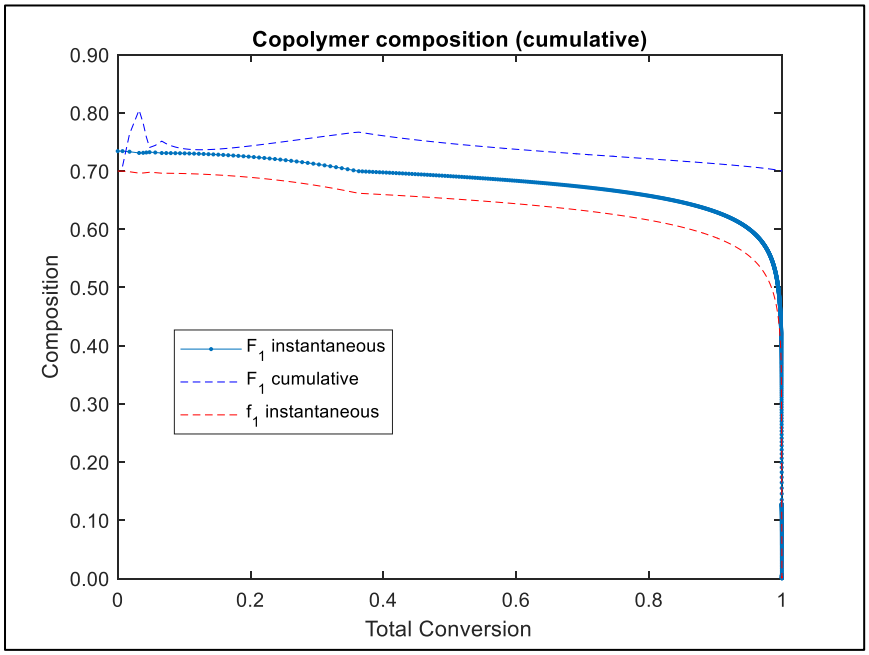

Figure XXXVIII - Copolymer cumulative composition in a semi-batch isothermal reactor affected by disturbances. As we may expect in this situation with this policy, the cumulative copolymer composition is not totally constant through all the reaction time due to the constantly monomer inflow variation of acrylamide at every time. Because the noise is relatively small, there is not great change in the cumulative composition.

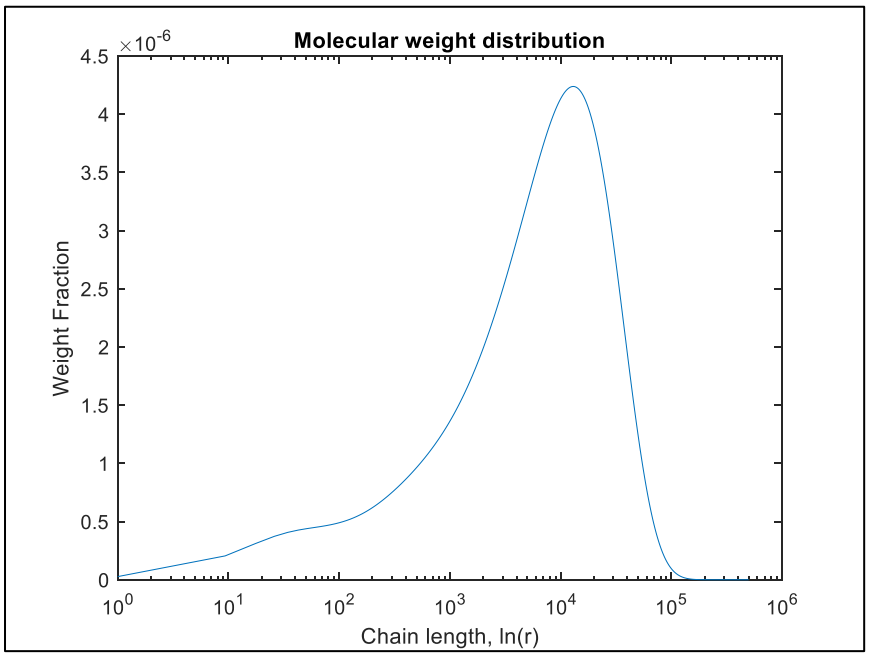

Figure XXXIX - Cumulative molecular weight distribution of the copolymer at full conversion for semi-batch isothermal conditions with disturbances. There is no major difference with the distribution for Case III.

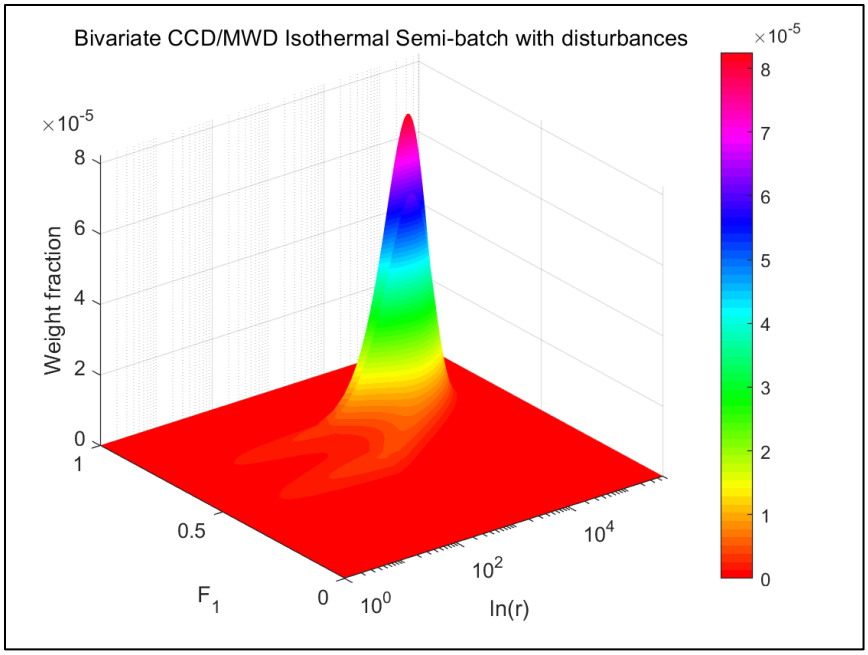

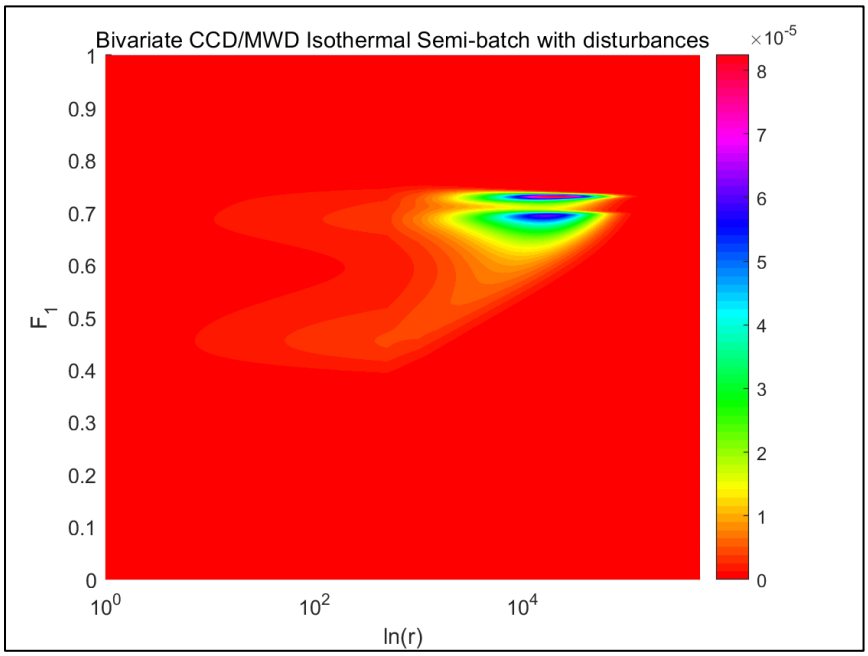

Figure XL and Figure XLI - Bivariate chemical composition/molecular weight distribution of the copolymer at full conversion. The copolymer composition has two peaks, both close to the desired copolymer composition of 0.7. The peaks are generated due to the inflow variation as function of time, which leads to random monomer concentration relations into the reactor but because the noise is small, they are closed to 0.7.

Case VI

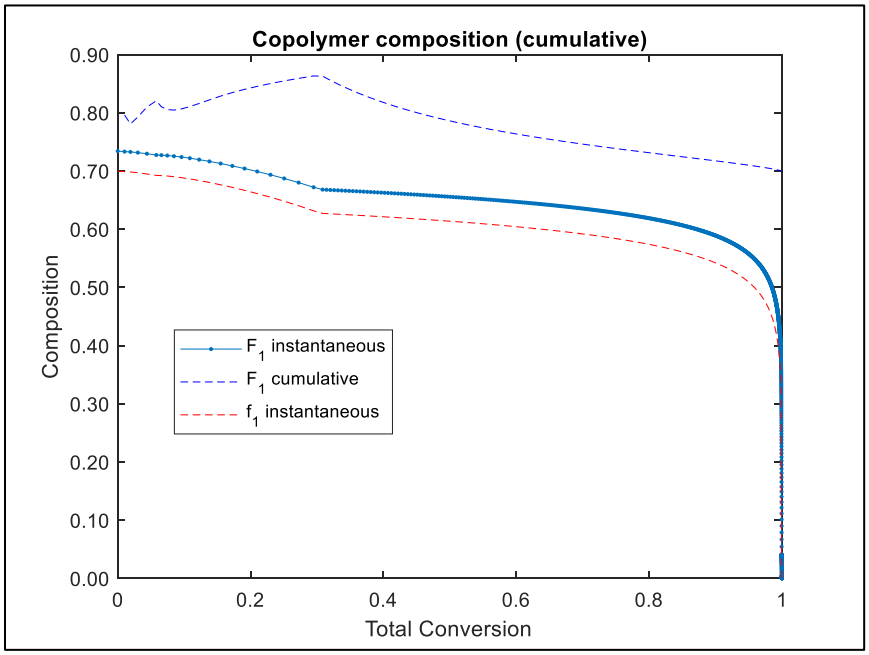

Figure XLII - Copolymer cumulative composition in a semi-batch isothermal reactor affected by disturbances. As we may expect in this situation with this policy, the cumulative copolymer composition is not totally constant through all the reaction time due to the constantly monomer inflow variation of acrylamide at every time. Because the noise is relatively small, there is not great change in the cumulative composition.

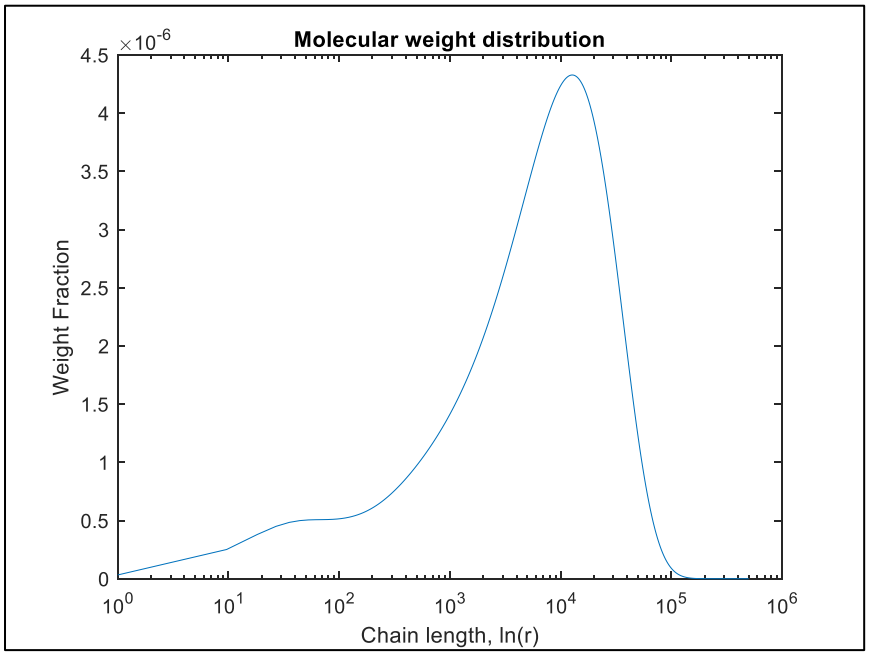

Figure XLIII - Cumulative molecular weight distribution of the copolymer at full conversion for semi-batch isothermal conditions with disturbances. There is no major difference with the distribution for Case III.

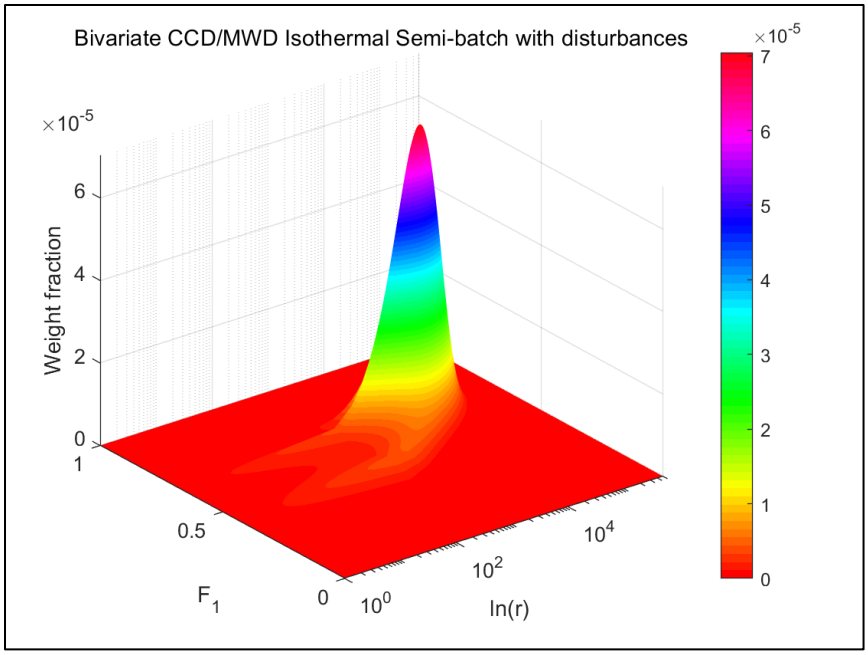

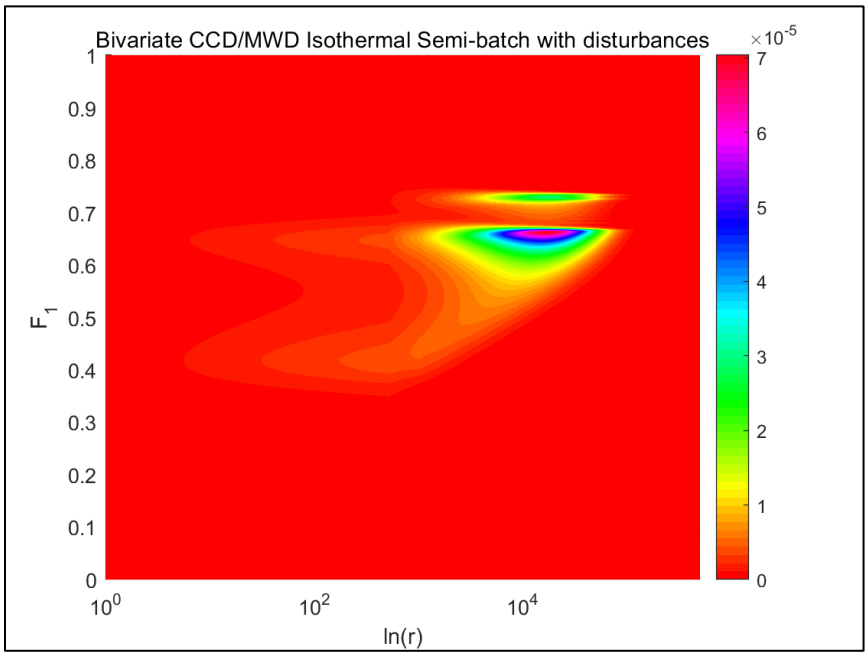

Figure XLIV and Figure XLV - Bivariate chemical composition/molecular weight distribution of the copolymer at full conversion. The copolymer composition has two clear peaks, both close to the desired copolymer composition of 0.7. The peaks are generated due to the inflow variation as function of time, which leads to random monomer concentration relations into the reactor, but because the noise is greater than Case V, they are a bit further from 0.7.

Case VI

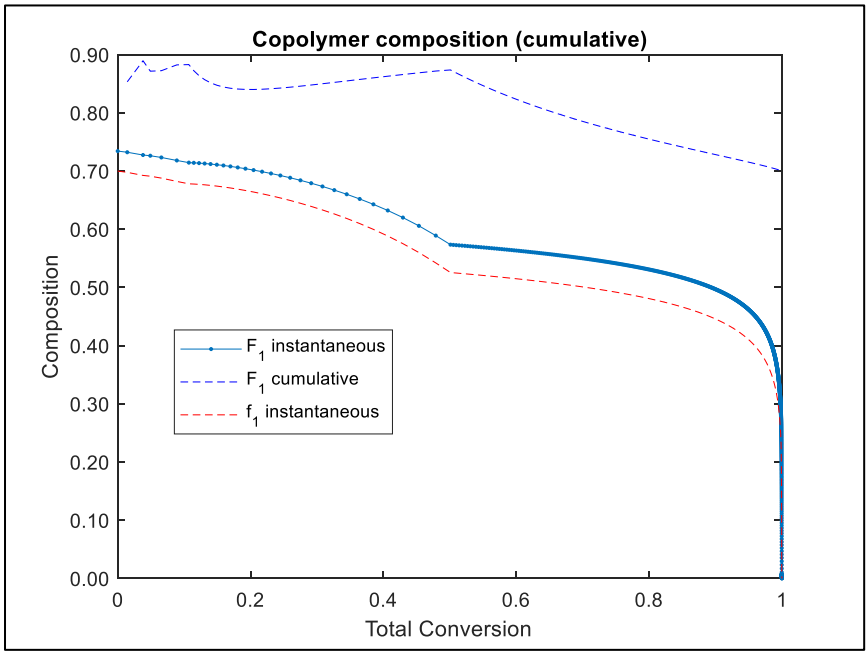

Figure XLVI - Copolymer cumulative composition in a semi-batch isothermal reactor affected by disturbances. As we may expect in this situation with this policy, the cumulative copolymer composition is not totally constant through all the reaction time due to the constantly monomer inflow variation of acrylamide at every time. Because the noise is greater than the other two cases, there are notable changes in the cumulative composition, especially at the beginning of reaction.

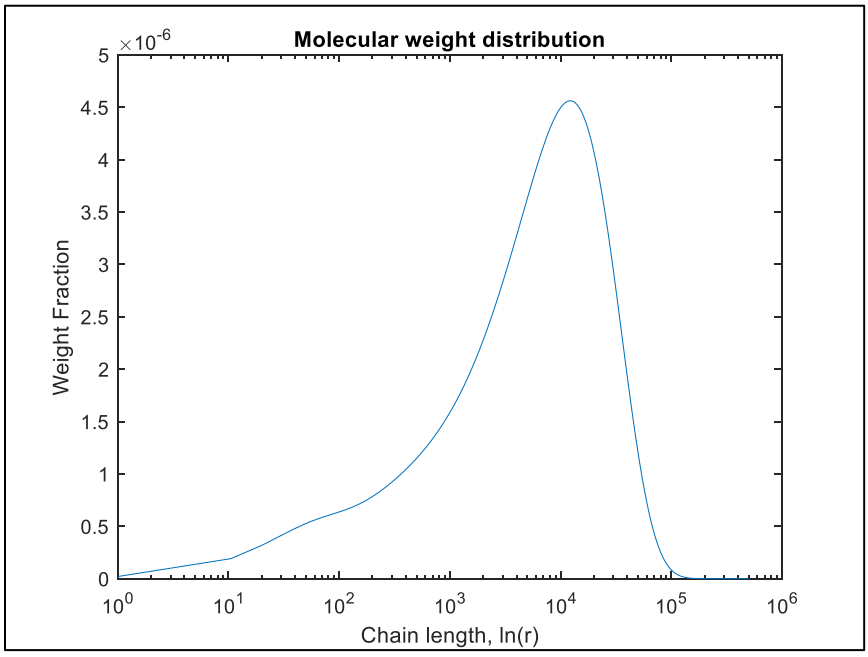

Figure XLVII - Cumulative molecular weight distribution of the copolymer at full conversion for semi-batch isothermal conditions with disturbances. There is no major difference with the distribution for Case III.

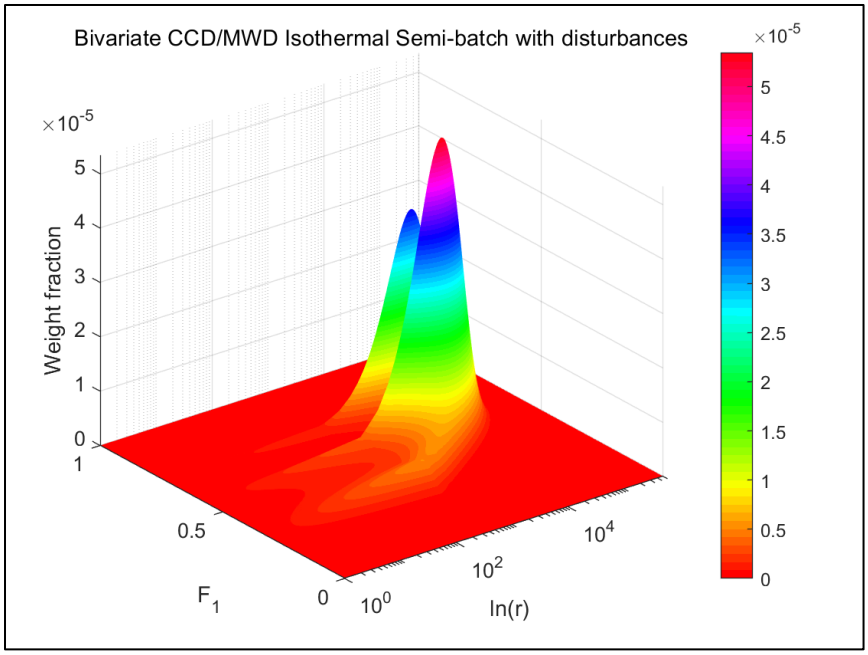

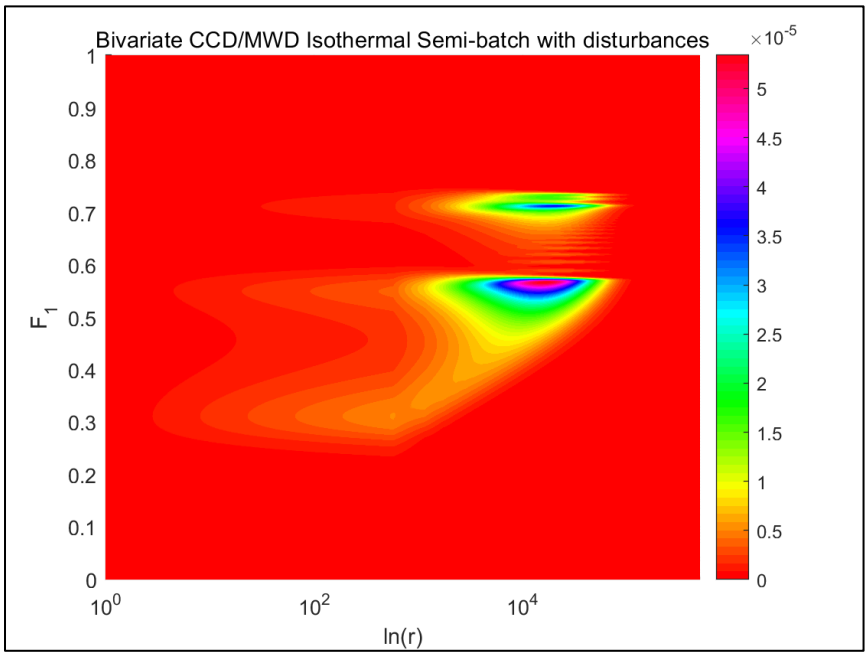

Figure XLVIII and Figure XLIX - Bivariate chemical composition/molecular weight distribution of the copolymer at full conversion. The copolymer composition has two clear peaks, both are much further to the desired copolymer composition of 0.7. The peaks are generated due to the inflow variation as function of time, which leads to random monomer concentration into the reactor. Because the concentration relations are close to the ideal relation, the peaks are relatively close to 0.7.

4.4. Part IV

Implementation and tuning of a PD controller

Reactor temperature is an important variable to control because it will directly affect the molecular weight distribution. If a narrow distribution in both copolymer composition and molecular weight is sought, Case III (Isothermal Semi-Batch) is the best alternative to select. Hence, temperature should be constant through the entire reaction and that implies the elimination of the heat generated by propagation reactions. So, based on Case IV temperature profile and the desired constant temperature in Case III, a PD controller for the non-isothermal semi-batch case has been implemented aiming to keep a constant temperature through all the reaction duration.

The PD controller equation could be expressed as following: [32]

$$u(t) = K_c\left[y_{sp}(t) - y_m(t)\right] + K_D\left(-\frac{dy_m}{dt}\right)$$

Where,

$u(t)$: controller output

K_C: proportional gain

K_D: derivative gain

$y_{sp}(t)$: variable setpoint at time t

$y_m(t)$: measured variable at time t

From the above equation we have tuned the gains to obtain a controller output that is not aggressive and assure a constant temperature at every time. In this case, we are supposing

that the reaction temperature is directed controlled but, in real process this parameter is directly related to a heat transfer process between the reactor, and the coolant temperature or flow rate.

Taking different values for the proportional and derivative gain we got the following controller output response:

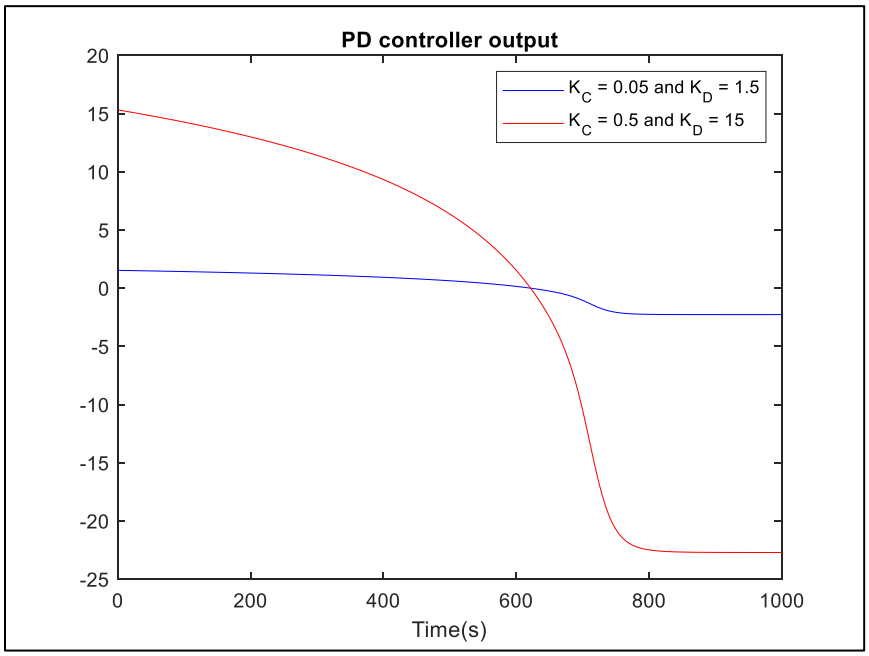

Figure L: PD output tuned to keep reactor temperature constant at every reaction time. As we can observe, larger values for the gains produce an output response that is more aggressive than the one for smaller values. Taking into consideration that those values could be percentage of a valve opening, when the profile takes smaller changes along the time, the system will not change a lot which make a better and more accurate prediction of the final microstructure.

5. Discussions

This discussion of the results will be centred in which reactor configuration could supply the best copolymer distribution in terms of both, composition and molecular weight at full monomer conversion. Also, we analyze how the different disturbances included in the system may affect the process and what changes in the final desired copolymer microstructure.

There are remarkable differences in the copolymer microstructure between the isothermal and adiabatic batch reaction conditions (Case I and II respectively). Firstly, the time reaction for the total conversion is longer in Case I than Case II. Although the initial temperatures in both situations were different, this rate of temperature increase is greater due to the heat released by the exothermic propagation reactions as the reaction advances. Higher temperatures lead to higher rate kinetic constants and therefore, monomers are consumed faster than Case I. Figure LI depicts the total monomer conversion as a function of time in both cases. As we can observe, the monomer conversion for Case I (Isothermal) at the beginning grows faster than Case II (Adiabatic) because the initial temperature is higher for Case I (Figure LII). Minutes later, when the temperature starts increasing due to the released reaction heat, the monomer consumption in Case II grows exponentially until some point where the conversion stays constant and close to 1. At that point, because the temperature is too high, the initiator does not tolerate the temperature anymore and it started disintegrating, which resulted in a reaction stop and consequently, the total conversion never reached 1.

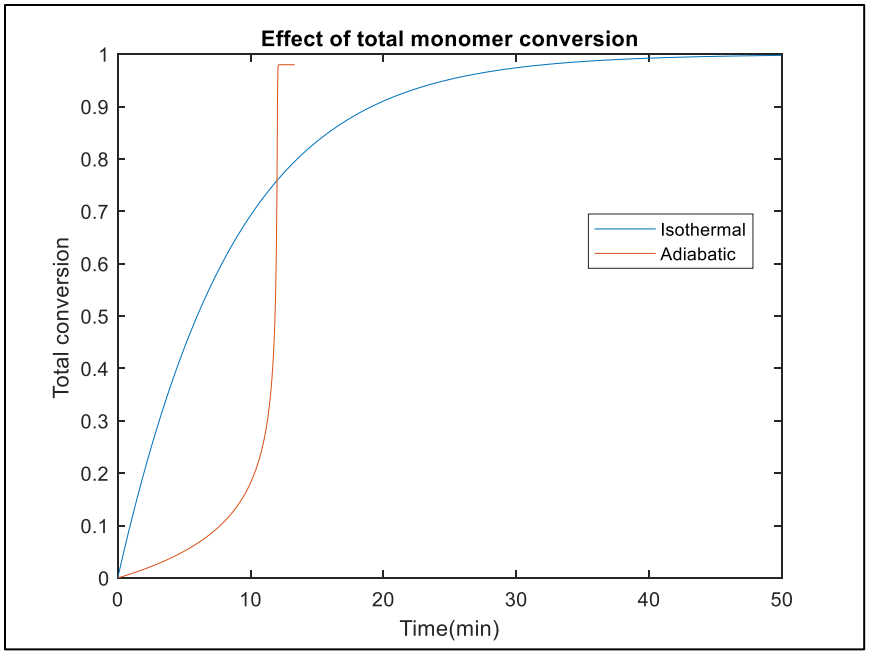

Figure LI – Comparison of the total monomer conversion as a function of time for both isothermal and adiabatic batch simulations.

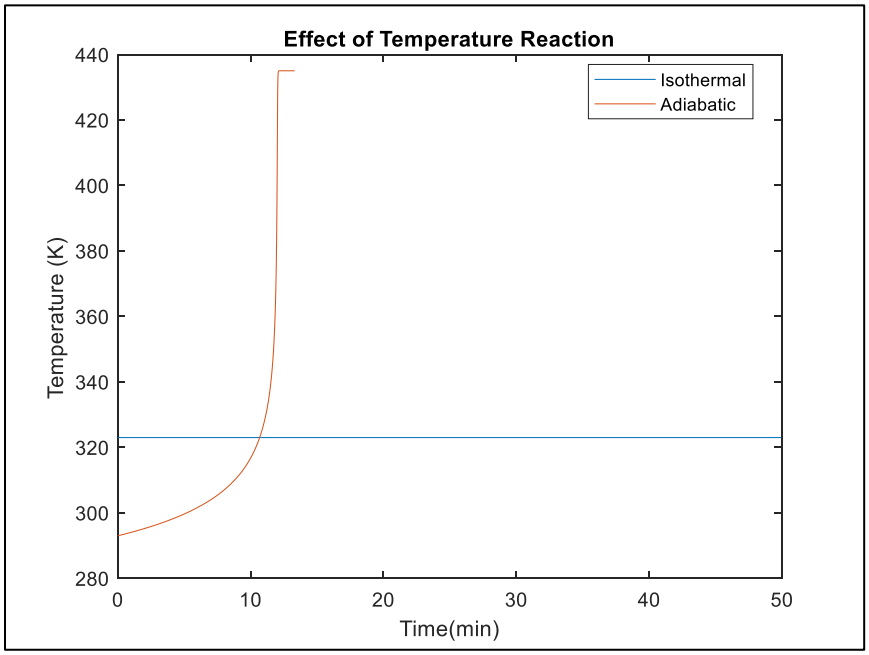

Figure LII – Comparison of the temperature reaction as a function of time for both isothermal and adiabatic batch conditions.

Other important properties that have shown remarkable variations when we move from Case I to Case II, are $\overline{M_n}$ and $\overline{M_w}$, and so PDI varies too. Figure LIII and Figure LIIIV depict the variation of those three parameters as a function of total conversion. We can conclude that there is no larger variation in the values of these parameters in Case I, which is consistent with the inverse proportion between the parameters and the reaction temperature. However, for Case II the temperature increases as the reaction advances, both number and molecular average weight decrease. This is because the length of a chain depends on the ratio $\frac{[M]}{[I]^{0.5}}$, and at a higher temperature, the monomer concentration decrease faster due to an increase in the global propagation constant which results in a lower $\overline{M_w}$. Figure VI – Cumulative molecular weight distribution of the copolymer at full conversion for isothermal conditions.Figure VI and Figure XV illustrate the cumulative molecular weight distribution at the end of reaction for both Case I and Case II respectively. We can observe from those that for Case I average copolymer weight $(\sim 10^4)$ is larger than Case II $(\sim 12^2)$. This is due to the reduction in the average molecular weight especially at higher conversions $(> 60\ \%)$, where the kinetic constants are higher and therefore the monomer concentration decreases faster and subsequently, the chain lengths produced from this point are smaller. This is also reflected in the value of the number and molecular average molecular weight which are decreasing as the reaction advances.

The bivariate copolymer composition distribution and molecular weight distribution at the end of reaction in both cases are completely different (Figure VII, Figure VII, Figure XVI and Figure XVI). In Case I a narrow distribution was achieved around the desired copolymer composition and the average molecular weight. However, this scenario is not the same in Case II

where the distribution for both copolymer composition and molecular weight is much broader and is not well-predicted, which directly affects the final physical copolymer properties.

Recalling the conclusions of Tobita, H. et al. (1991), the PKRCM has an error of less than 5 % when the average molecular weight is equal or greater than 103. In Case II the average molecular weight is between 102 and 103, which could be an important source of error when is compared with the results of a real adiabatic batch copolymerization. So, based on both the copolymer microstructure mentioned before and the error associated with the PKRCM method, isothermal batch (Case I) is a much better configuration to produce the desired copolymer.

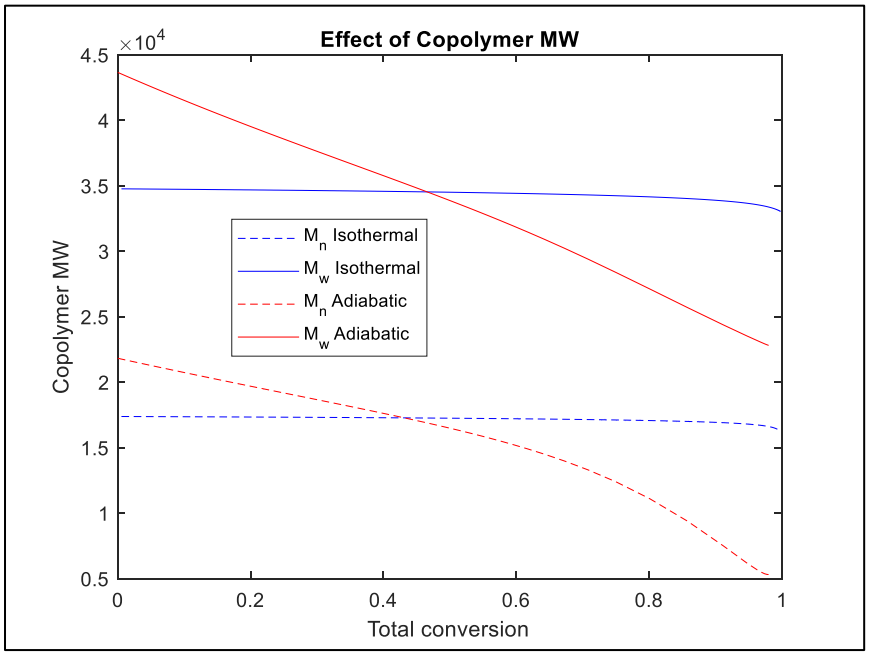

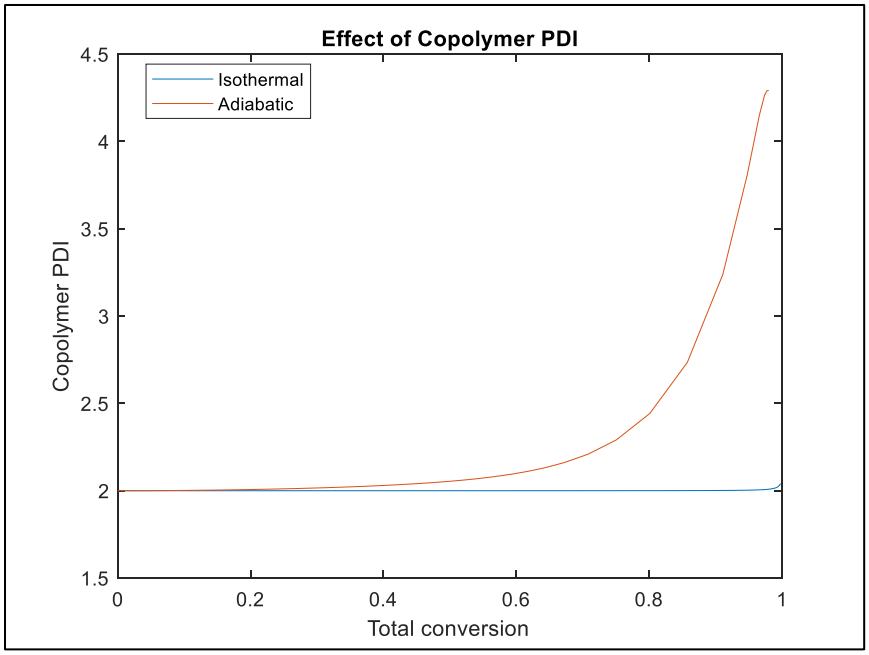

Figure LIII and Figure LIV – Top: Comparison between the number and molecular average cumulative molecular weight as a function of total monomer conversion. Bottom: PDI variation for both Case I and Case II as a function of the total conversion.

Major insights can be gleaned from an analysis of the differences between Case III and Case IV. Firstly, Figure LV illustrates the comparison of the total conversion as a function of time for both cases. Total conversion in Case III is faster at the beginning of reaction than the other case due to the initial higher temperature. Later, because the temperature in Case IV starts growing quickly, the conversion profile is almost exponential and full conversion is reached before.

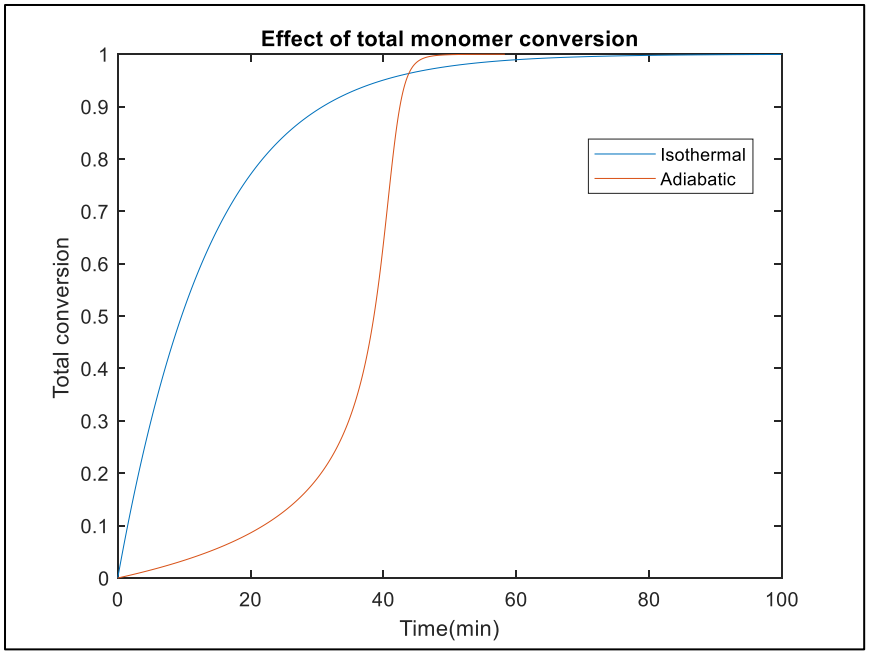

Figure LV - Comparison of the total monomer conversion as a function of time for both Case III and Case IV.

Secondly, the number and molecular average molecular weight are almost constant for Case III at every point in time but decrease for both parameters in Case IV due to the temperature variation. As we mentioned before, the temperature increases as the reaction proceeds, the propagation kinetic constants are larger and therefore, the monomer concentration is reduced faster. This leads to the formation of chains with smaller length especially at higher conversions which are reflected in the constant reduction of both $\overline{M_n}$ and $\overline{M_w}$ as the reaction advances. So, PDI varies for Case IV and is practically constant in Case III. Figure LVI and Figure LVI depict the variation for these values in the two cases. Considering all the cases, the PDI in Case I and III is the same which is to be expected because it is an isothermal system. Although the PDI variation in Case II and IV are similar, Case II reaches a higher value at the end of reaction because of the greater final reaction temperature compared to Case IV.

A very important difference between Case III and IV is the molecular weight distribution at the end of reaction. From Figure XXIII and Figure XXXII if a narrow molecular weight distribution is sought, we may conclude that a temperature variation is not a desired factor in the process due to the much broader distribution found in Case IV. This is related to the reasons mentioned before in the kinetic constant variations.

Although the copolymer composition across all the molecular weights is the one desired (Figure XXXIII), the copolymer produced at the end of reaction has a lower average molecular weight and a wider distribution of different chain lengths. Nonetheless, as you may observe in Figure XXIV, Case III has the best narrow distribution in terms of both, copolymer composition and molecular weight distribution which was the expected. There are two reasons for this: First, the monomer relation in the reaction mixture is kept constant throughout the entire reaction and second, the isothermal condition is conducive to a narrow distribution of the molecular weights.

Moreover, considering all the cases and conditions and what we expect from a copolymer microstructure, the best configuration to carry out the production of a copolymer is Case III, where a very narrow distribution was achieved for both copolymer composition and molecular weight distribution. In addition, the average molecular weight is greater than 10^3, which is limits errors in the model due to the PKRMC limitations. Because one of the objectives of this project is to simulate real scenarios in the industry, we know that constant inflows may not be possible to obtain, and that any system generates natural disturbances that make Case III too ideal in terms of implementation.

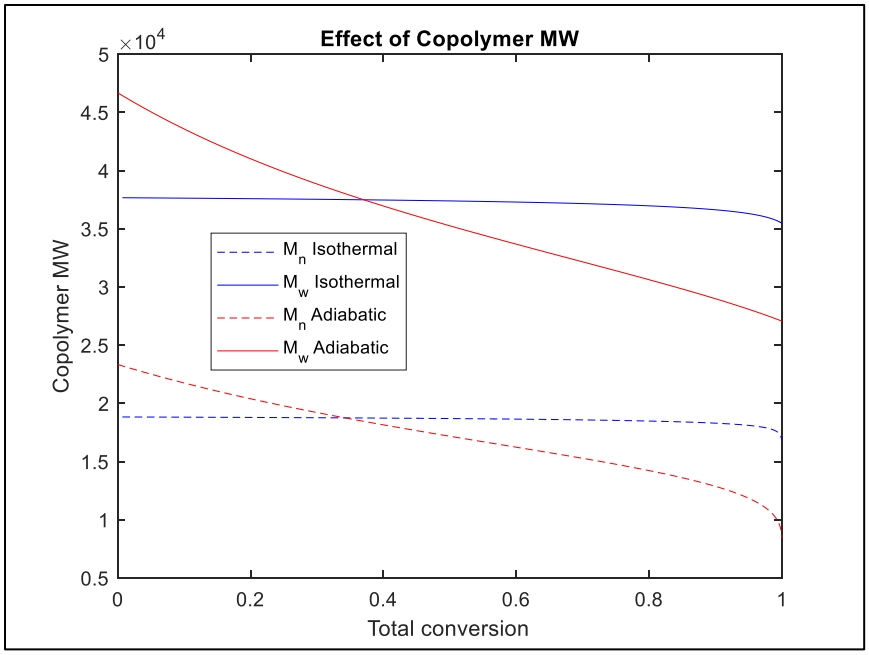

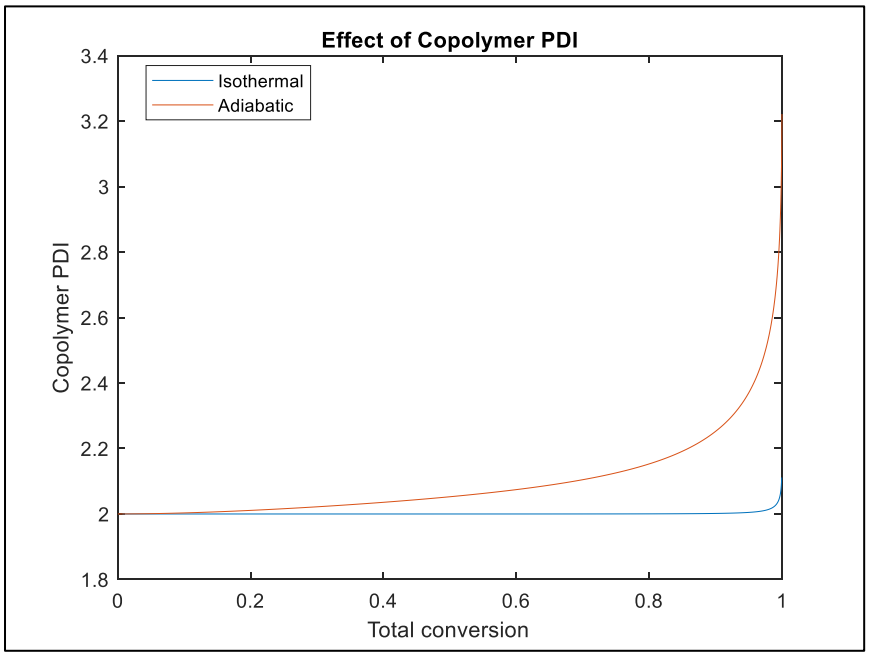

Figure LVI and Figure LVII – Top: Comparison between the number and molecular average cumulative molecular weight as a function of total monomer conversion. Bottom: PDI variation for both Case III and Case IV as a function of the total conversion.

In order of considering a possible real case in the industry, we have added a white noise signal as disturbances into the necessary acrylamide inflow to obtain the same copolymer that in Case III. We now discuss how the presence of disturbances affects the final copolymer

microstructure. Figure XXXVIII shows the cumulative copolymer composition as a function of total conversion, which is not constant due to the white noise in the inflow. Hence, the cumulative composition is unpredictable and varied. Since the white noise standard deviation is relatively small for Case V, the average composition still hews closely to the desired value. Once the standard deviation is increased (Figure XLII and Figure XLVI) the cumulative composition at the beginning of the reaction is higher but then it tends to reach the desired value at full conversion. Because of the disturbance presence, the cumulative composition is not constant at any time of the semi-batch operation, which has a considerable impact on the copolymer composition distribution. Figure XL, Figure XLIV and Figure XLVIII depict the significant impact that the disturbance on various parameters as the variance of the white noise grows. For example, even though for Case V we have a relatively small value, the final copolymer composition is like Case I (isothermal batch reactor), where we may detect the presence of two maxima located closely to the desired monomer composition value. As the variance increases, the peaks get further from 0.7 and the difference between them and the copolymer obtained in Case III is clear. The peak formation for each of the Cases is due to the random monomer inflow rate into the reaction mixture, which is no longer properly pointed to get a copolymer with that specific monomer composition. Because those signals are uncorrelated random values with zero mean and finite variance, at every time, the inflow rate randomly varies along with the required monomer inflow. Then, the inflow could or could not be the exact value calculated in Case III to produce a copolymer with constant monomer composition and avoid drifts. The molecular weight distribution for the three cases with disturbance are analogous and share almost the same

distribution. That is because the temperature is constant, and the monomer concentration relation does not drastically affect the average copolymer chain length at the final conversion.

Finally, PD controller shows a different output profile when the proportional and derivative gains are changed. Those changes are depicted in Figure L. Taking into consideration that controller outputs are the system inputs, a predicted input profile close to zero means that there will not be a great variation in the system. Since we are considering that only reaction temperature is controlled, the controller that have less aggressive response should be selected. In our case, those values could be K_C: 0.05 and K_D: 1.5.

6. Conclusions

A mathematical model for the free radical copolymerization between acrylamide and acrylic acid has been developed. The simulations of various reactor configurations that are often found in industry were carried out, considering batch, semi-batch, isothermal and adiabatic conditions. Afterwards, the final copolymer microstructure for each situation was predicted based on the simplifications stated before, such as considering that only linear polymer chains form, absence of some chemical reactions and components like chain transfer agents and the certain limitations of PKRCM. Of course, those assumptions could be accounted by including the rate expressions and component balances. However, for this work, the results obtained for almost all the cases except for Case II are within an error of less than 5 % based on Tobita, H. et al. (1991). If a very narrow bivariate distribution for both the copolymer composition and the molecular weight is sought, then the semi-batch isothermal reactor (Case III) is the best configuration to carry out copolymer production. Because of this, white noise with different

variances was added on to this inflow profile, and its final microstructure was then estimated. Based on the above results and discussions, white noise with a small variance such as 0.10 may have a significant influence in the final copolymer properties, especially in the final monomer relation leading to an undesired composition drift. At higher variances, there will be greater deviation from the expected microstructure that could lead to the semi-batch isothermal configuration becoming impractical for to obtain specific copolymer microstructures. Finally, a PD controller was implemented to ensure that the temperature will be constant through the whole reaction which will ensure that expected narrow distribution for both copolymer composition and molecular weight distributions.

7. References

[1] Asua José M. Polymer Reaction Engineering. Blackwell Pub., 2007.

[2] Dubé, Marc A., et al. “Mathematical Modeling of Multicomponent Chain-Growth Polymerizations in Batch, Semibatch, and Continuous Reactors: A Review.” Industrial & Engineering Chemistry Research, vol. 36, no. 4, 1997, pp. 966–1015., doi:10.1021/ie960481o.

[3] Hamer, J.W., et al. “The Dynamic Behavior of Continuous Polymerization Reactors—II Nonisothermal Solution Homopolymerization and Copolymerization in a CSTR.” Chemical Engineering Science, vol. 36, no. 12, 1981, pp. 1897–1914., doi:10.1016/0009-2509(81)80029-2.

[4] Broadhead, T. O., et al. “Dynamic Modelling of the Batch, Semi-Batch and Continuous Production of Styrene/Butadiene Copolymers by Emulsion Polymerization.” Die Makromolekulare Chemie, vol. 10, no. S19851, 1985, pp. 105–128., doi:10.1002/macp.1985.020101985110.

[5] Hamielec, A. E., et al. “Multicomponent Free-Radical Polymerization in Batch, Semi- Batch and Continuous Reactors.” Makromolekulare Chemie. Macromolecular Symposia, vol. 10-11, no. 1, 1987, pp. 521–570., doi:10.1002/masy.19870100126.

[6] Tobita, Hidetaka, and Archie E. Hamielec. “Kinetics of Free-Radical Copolymerization: the Pseudo-Kinetic Rate Constant Method.” Polymer, vol. 32, no. 14, 1991, pp. 2641–2647., doi:10.1016/0032-3861(91)90345-j.

[7] Xie, Tuyu, and Archie E. Hamielec. “Modelling Free-Radical Copolymerization Kinetics, Molecular Weight Calculations for Copolymers with Crosslinking.” Die Makromolekulare Chemie, Theory and Simulations, vol. 2, no. 5, 1993, pp. 777–803., doi:10.1002/mats.1993.040020513.

[8] Riahinezhad, Marzieh, et al. “Optimal Estimation of Reactivity Ratios for Acrylamide/Acrylic Acid Copolymerization.” Journal of Polymer Science Part A: Polymer Chemistry, vol. 51, no. 22, Feb. 2013, pp. 4819–4827., doi:10.1002/pola.26906.

[9] Abdel-Alim, A. H., and A. E. Hamielec. “Shear Degradation of Water-Soluble Polymers. I. Degradation of Polyacrylamide in a High-Shear Couette Viscometer.” Journal of Applied Polymer Science, vol. 17, no. 12, 1973, pp. 3769–3778., doi:10.1002/app.1973.070171218.

[10] Zaitoun, Alain, et al. “Shear Stability of EOR Polymers.” SPE International Symposium on Oilfield Chemistry, 2011, doi:10.2118/141113-ms.

[11] Vedoy, Diógenes R. L., and João B. P. Soares. “Water-Soluble Polymers for Oil Sands Tailing Treatment: A Review.” The Canadian Journal of Chemical Engineering, vol. 93, no. 5, 2015, pp. 888–904., doi:10.1002/cjce.22129.

[12] Kattner, Hendrik, and Michael Buback. “Termination and Transfer Kinetics of Acrylamide Homopolymerization in Aqueous Solution.” Macromolecules, vol. 48, no. 20, June 2015, pp. 7410–7419., doi:10.1021/acs.macromol.5b01921.

[13] Penlidis, A., et al. “Dynamic Modeling of Emulsion Polymerization Reactors.” AIChE Journal, vol. 31, no. 6, 1985, pp. 881–889., doi:10.1002/aic.690310602.

[14] Ray, W. Harmon. “On the Mathematical Modeling of Polymerization Reactors.” Journal of Macromolecular Science, Part C, vol. 8, no. 1, 1972, pp. 1–56., doi:10.1080/15321797208068168.

[15] Rawlings, J. B., and W. H. Ray. “The Modeling of Batch and Continuous Emulsion Polymerization Reactors. Part I: Model Formulation and Sensitivity to Parameters.” Polymer Engineering and Science, vol. 28, no. 5, 1988, pp. 237–256., doi:10.1002/pen.760280502.

[16] Kiparissides, C., et al. “Continuous Emulsion Polymerization. Modeling Oscillations in Vinyl Acetate Polymerization.” Journal of Applied Polymer Science, vol. 23, no. 2, 1979, pp. 401–418., doi:10.1002/app.1979.070230210.

[17] Hawker, Craig J., et al. “New Polymer Synthesis by Nitroxide Mediated Living Radical Polymerizations.” Chemical Reviews, vol. 101, no. 12, 2001, pp. 3661–3688., doi:10.1021/cr990119u.

[18] Preusser, Calista, et al. “The Combined Influence of Monomer Concentration and Ionization on Acrylamide/Acrylic Acid Composition in Aqueous Solution Radical Batch Copolymerization.” Macromolecules, vol. 49, no. 13, 2016, pp. 4746–4756., doi:10.1021/acs.macromol.6b00919.

[19] Rintoul, Ignacio, and Christine Wandrey. “Polymerization of Ionic Monomers in Polar Solvents: Kinetics and Mechanism of the Free Radical Copolymerization of Acrylamide/Acrylic Acid.” Polymer, vol. 46, no. 13, 2005, pp. 4525–4532., doi:10.1016/j.polymer.2005.04.005.

[20] Ponratnam, Surendra, and Sham Lal Kapur. Die Makromolekulare Chemie, vol. 178, no. 4, 1977, pp. 1029–1038., doi:10.1002/macp.1977.021780408.

[21] Truong, N.d., et al. “Microstructure of Acrylamide-Acrylic Acid Copolymers: 1. As Obtained by Alkaline Hydrolysis.” Polymer, vol. 27, no. 3, 1986, pp. 459–466., doi:10.1016/0032-3861(86)90166-7.

[22] Truong, N.d., et al. “Microstructure of Acrylamide-Acrylic Acid Copolymers: 2. As Obtained by Direct Copolymerization.” Polymer, vol. 27, no. 3, 1986, pp. 467–475., doi:10.1016/0032-3861(86)90167-9.

[23] Shawki, S. M., and A. E. Hamielec. “Estimation of the Reactivity Ratios in the Copolymerization of Acrylic Acid and Acrylamide from Composition–Conversion Measurements by an Improved Nonlinear Least-Squares Method.” Journal of Applied Polymer Science, vol. 23, no. 11, Jan. 1979, pp. 3155–3166., doi:10.1002/app.1979.070231102.

[22] Cabaness, W. R., et al. “Effect of PH on the Reactivity Ratios in the Copolymerization of Acrylic Acid and Acrylamide.” Journal of Polymer Science Part A-1: Polymer Chemistry, vol. 9, no. 8, 1971, pp. 2155–2170., doi:10.1002/pol.1971.150090805.

[23] Mayo, Frank R., and Frederick M. Lewis. “Copolymerization. I. A Basis for Comparing the Behavior of Monomers in Copolymerization; The Copolymerization of Styrene and Methyl Methacrylate.” Journal of the American Chemical Society, vol. 66, no. 9, 1944, pp. 1594–1601., doi:10.1021/ja01237a052.

[24] Kuo, Jen-Feng, and Chuh-Yung Chen. “Studies on the Radical Chain Copolymerization of Methyl Methacrylate and Styrene at Their Azeotropic Composition.” Macromolecules, vol. 14, no. 2, 1981, pp. 335–339., doi:10.1021/ma50003a021.

[25] Xie, T.y., et al. “Experimental Investigation of Vinyl Chloride Polymerization at High Conversion: Molecular-Weight Development.” Polymer, vol. 32, no. 6, 1991, pp. 1098–1111., doi:10.1016/0032-3861(91)90599-e.

[26] Stockmayer, W. H. “Distribution of Chain Lengths and Compositions in Copolymers.” The Journal of Chemical Physics, vol. 13, no. 6, 1945, pp. 199–207., doi:10.1063/1.1724022.

[27] Tacx, J. C. J. F., et al. “Effect of Molar Mass Ratio of Monomers on the Mass Distribution of Chain Lengths and Compositions in Copolymers: Extension of the Stockmayer Theory.” Journal of Polymer Science Part A: Polymer Chemistry, vol. 26, no. 1, 1988, pp. 61–69., doi:10.1002/pola.1988.080260106.

[28] Wittenberg, Nils F. G., et al. “Modeling Acrylic Acid Radical Polymerization in Aqueous Solution.” Macromolecular Reaction Engineering, vol. 10, no. 2, Nov. 2015, pp. 95–107., doi:10.1002/mren.201500017.

[29] Preusser, Calista, et al. “Modeling the Radical Batch Homopolymerization of Acrylamide in Aqueous Solution.” Macromolecular Reaction Engineering, vol. 10, no. 5, 2016, pp. 490–501., doi:10.1002/mren.201500076.

[30] Evans, Alwyn G., and E. Tyrrall. “Heats of Polymerization of Acrylic Acid and Derivatives.” Journal of Polymer Science, vol. 2, no. 4, 1947, pp. 387–396., doi:10.1002/pol.1947.120020404.

[31] Thomson, R. A. M. “A Kinetic Study of the Adiabatic Polymerization of Acrylamide.” Journal of Chemical Education, vol. 63, no. 4, 1986, p. 362., doi:10.1021/ed063p362.

[32] Seborg, D. E., et al. Process Dynamics and Control. Wiley, 2004.